The Vulnerability of U.S. Coastal Energy Infrastructure Under Climate Change

by

Megan Jeramaz Lickley

Submitted to the Department of Engineering Systems Division
in partial fulfillment of the requirements for the degree of

Master's of Science in Technology and Policy

at the

MASSACHUSETTS INSTITUTE OF TECHNOLOGY

September 2012

Author .....
Department of Engineering Systems Division
August 10, 2012

Certified by .....
Professor Henry D. Jacoby
Professor of Management, Sloan School of Management
Thesis Supervisor

Accepted by .....
Joel P. Clark
Professor of Materials Systems and Engineering Systems
Acting Director, Technology & Policy Program

The Vulnerability of U.S. Coastal Energy Infrastructure Under Climate Change

by

Megan Jeramaz Lickley

Submitted to the Department of Engineering Systems Division
on August 10, 2012, in partial fulfillment of the
requirements for the degree of
Master's of Science in Technology and Policy

Abstract

The 2005 hurricane season was particularly damaging to the United States, contributing to significant losses to energy infrastructure –much of it a result of flooding from storm surges during hurricanes Katrina and Rita. Previous research suggests that these events are not isolated, but rather foreshadow a risk that is to continue and likely increase with a changing climate (17). Since extensive energy infrastructure exists along the U.S. Atlantic and Gulf coasts, these facilities are exposed to an increasing risk of flooding. We study the combined impacts of anticipated sea level rise, hurricane activity, and subsidence on energy infrastructure in these regions with a first application to Galveston Bay. Using future climate conditions as projected by four different Global Circulation Models (GCMs), we model the change in hurricane activity from present day climate conditions in response to a climate projected in 2100 under the IPCC A1B emissions scenario using hurricane analysis developed by Emanuel (5). We apply the results from hurricane runs from each model to the SLOSH model (Sea, Lake and Overland Surges from Hurricanes) (19) to investigate the change in frequency and distribution of surge heights across climates. Further, we incorporate uncertainty surrounding the magnitude of sea level rise and subsidence, resulting in more detailed projections of risk levels for energy infrastructure over the next century. With a detailed understanding of energy facilities' changing risk exposure, we conclude with a dynamic programming cost-benefit analysis to optimize decision making over time as it pertains to adaptation.

Thesis Supervisor: Professor Henry D. Jacoby
Title: Professor of Management, Sloan School of Management

Acknowledgments

I am extremely thankful to my thesis supervisor, Jake Jacoby. He has been ever patient with me, attentive to every detail of my work, and an extremely encouraging and dedicated supervisor. It has been a pleasure working with him and I truly appreciate the amount of time he has dedicated to my project.

Next, I'd like to acknowledge the work provided by Professor Kerry Emanuel and Dr. Ning Lin. My research has been largely based on their hurricane and storm surge analysis. I would like to add that they have not yet seen the work that I have documented here and that I take full responsibility should I have misrepresented their methodology or the results of their analysis.

To the professors, peers, and staff at the Join Program on the Science and Policy of Global Change; I am grateful to have had the opportunity to work beside you all. Thank you for all of your support and guidance throughout my research.

My time at MIT and in the Technology and Policy Program has been an exceptional experience. I would like to extend my gratitude towards my fellow grad students, professors, and mentors along the way who have provided me with friendship, guidance, and much much inspiration.

To my family and friends; your endless encouragement continues to be a pillar in my life.

Lastly, I would like to gratefully acknowledge the financial support for this work provided by the MIT Joint Program on the Science and Policy of Global Change through a consortium of industrial sponsors and Federal grants, with special gratitude for support from the U.S. Department of Energy, Office of Science (DE-FE02-94ER61937).

Contents

List of Figures

List of Tables

Chapter 1

The Increased Risk of Coastal Flooding

Major hurricanes in recent years have threatened energy security in the United States. Hurricane Katrina in August of 2005, followed by Hurricane Rita in September, delivered the 'world's first integrated energy shock' as it simultaneously disrupted oil, natural gas, and electric power generation, halting 27 percent of U.S. oil production and 21 percent of U.S. refining capacity (33). A large portion of this damage was a result of flooding from storm surges which reached heights as high as 8.5 m on the open coast (9). The incredible loss from these storms raises the question: Are these isolated events or are hurricanes becoming more destructive in a changing climate? This work aims to answer that question. More specifically, we focus on the damage that coastal energy infrastructure is exposed to under climate change. Further, we expand from these risk exposures to capture the expected benefit and optimal timeframe for adaptation. For coastal infrastructure at risk of flooding, adaptation involves protective levees built to retain ocean water. The cost of constructing and maintaining the levees is weighed against the expected damage costs of postponing precautionary adaptation measures. We present a time-dependent dynamic decision making process built to minimize the expected costs.

1.1 Climate Change

Anthropogenic greenhouse gas emissions have lead to an increased concentration of greenhouse gases in the atmosphere. Carbon dioxide, for instance, has increased by 31% since

preindustrial times (13). The presence of greenhouse gases in the atmosphere traps outgoing radiation. Without these gases, Earth would be inhabitable; however, an increased concentration of greenhouse gases over the past century has resulted in an increase in global temperatures and thus a changing climate. As anthropogenic greenhouse gas emissions continue to increase in concentration, we expect to see global average temperatures increase further. The rate of this increase is largely dependent on the rate of emissions as well as the feedback loops that occur (28). This past century, global average temperatures have risen by 0.8^{o}C with about 0.6^{o}C of that increase occurring since 1980 (23). The IPCC AR4 report predicts this trend of temperature increases to continue and to be another 0.3 to 6.4 ^{o}C higher by the year 2100 (28).

This increase in temperature that we have seen over the past three decades has had a variety of effects on our global environmental system. Increases in atmospheric water vapor, increases in ocean temperatures, decreases in glacial snow cover and arctic sea ice, and changes in precipitation are among many of the changes that have been recorded over the past several decades (2). Most relevant to this project are the changes in tropical storm activity and sea level rise, which also happen to be the two areas of climate science with some of the greatest uncertainty. While a geographic location may see a wide range of storms every year, damage to infrastructure is generally all accounted for during the rare severe storms. Recently, studies have shown that 10% of storms cause 90% of damage, and 1% of storms cause 58% of damage globally. Under climate change, the intensity of severe storms is anticipated to increase with estimates suggesting 10% of storms will cause 93% of damage and 1% of storms will cause 64% of damages (31). Speculation about an increase in intensity of extreme storm events is based on the understanding that with an increase in sea surface temperature (SST), tropical storms will have more potential to grow in intensity and develop to be more destructive (18).

Increased temperatures have also affected ocean levels and are anticipated to affect them further in the future. Cazenave and Llovel estimate that the mean sea level has risen about 17cm since 1900 as a result of increased global temperatures (3). Global temperatures affect ocean levels in two distinct ways. One is through thermal expansion: As ocean temperatures increase, water expands, taking up more space and increasing sea level. The

second is through a decrease in land-ice cover leading to more water running off into the oceans. Scientists have a fairly good idea of the temperature effects on thermal expansion, temperature impacts on the melting rate of the great ice sheets is a less understood relationship.

Understanding the physical processes that lead to the observed trends in sea level rise and hurricane frequency and intensity helps us to predict a future climate scenario.

1.2 Energy Facilities at Risk

The United States, as the third largest oil producer in the world, second largest producer of natural gas, and second largest producer of coal, necessarily has a large amount of energy infrastructure. With a changing climate, infrastructure is exposed to more extremes, most destructive being extreme wind and water damage. While wind has destructive potential for power lines and window damage, large scale energy infrastructure is most vulnerable to damage resulting from floods. This reduces the scope of facilities at risk under consideration here to those at risk of flooding. To further reduce our scope, we focus our analysis specifically on coastal flooding. In the United States, coastal energy infrastructure is largely a mix of oil refineries, oil import sites, and natural gas hubs (29). Much of this infrastructure is on the Atlantic Coast and Gulf Coast of the U.S., with the Gulf Coast being more densely populated with these facilities. The Eastern side of the U.S. also happens to be exposed to North Atlantic Tropical Cyclones. As an example of the facilities at risk, Figure 1-1 shows the distribution of electric generation in the U.S..

1.3 Components of Climate Change Risk

Considering coastal energy infrastructure, we examine the range of factors that lead to a change in risk. As the 2005 hurricane season indicated, energy infrastructure is vulnerable to storm surges from the North Atlantic Hurricane season. Under climate change, the potential for extreme storm surges is liable to increase. A rising sea level is another contributing factor to vulnerability change. Further, as a result of ground water extraction

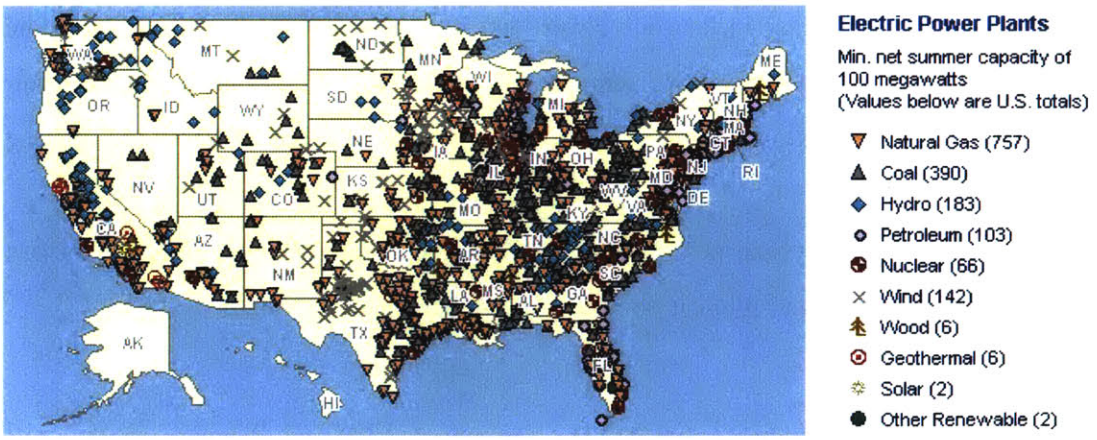

Figure 1-1: Electric Power Plants in the United States (http://www.eia.gov/state/)

and the extraction of other mined resources, many locations are experiencing subsidence. These are the factors accounted for in our risk assessment.

1.3.1 Hurricane Intensity and Surge

Atlantic Hurricanes

According to the National Oceanic and Atmospheric Administration (NOAA), each year approximately ten tropical storms develop in the North Atlantic, Caribbean, and Gulf of Mexico, six of which develop into hurricanes, of which only one or two make landfall (1). A hurricane is defined as 'an intense tropical weather system of strong thunderstorms with a well-defined surface circulation and maximum sustained winds of 74 mph or higher' (1). Hurricanes are on average 300 miles wide, and they generally survive for 2 weeks. In order to form, hurricanes require pre-existing weather disturbances, atmospheric moisture, warm ocean water (80^{o}F or higher), and light prevailing winds.

Typically, under these conditions, a cluster of thunderstorms grows in the middle of the Atlantic, continually feeding off the warmth of the ocean water and the heat that is produced as water vapor condenses into drops. Strong prevailing winds can often tear these tropical depressions apart; however, with light prevailing winds the tropical depression will move and, with the Coriolis effect, begin the counterclockwise rotation and take on the typical spiral formation. At this point, what was originally a tropical depression has reached the

classification of a tropical storm. If the storm continues to grow and become strong enough (winds 74 mph or higher), the storm is classified as a hurricane. If, however, the storm passes over cooler bodies of water or over land, it will lose energy and die off.

The Saffir-Simpson scale is a popular scale that was introduced by wind engineer Herb Saffir and meteorologist Bob Simpson as a means of communicating the severity of storms. It assigns storms to categories 1 through 5, based solely on the maximum windspeed of the storm. This measure has been somewhat effective in providing warnings of the severity of a storm but it neglects to describe a variety of factors that can have great influence over the gravity of the hurricane such as size and direction of approach. While windspeed is generally an indication of how much wind-damage a storm can produce, maximum windspeed only describes part of a hurricane's intensity. Alternatives to the Saffir-Simpson scale have been introduced such as the Power Dissipation Index used by Emanuel (4):

$$PDI = \int V_{max}^3 dt, \tag{1.1}$$

where V_{max}^3 is the maximum wind speed and the interval is over the lifetime of the storm. Emanuel was able to show a correlation between SST and PDI for North Atlantic storms from 1930 to 2005 (see Figure 1-2)(4). This work shows that Atlantic PDI has more than doubled since 1975 as temperatures have increased by about 0.5^oC.

But Emanuel stresses that SST alone cannot explain the increase in the destruction potential of hurricanes. He points to other contributing factors such as the entire temperature profile of the troposphere and vertical wind shear. There is evidence that an increase in global temperatures also contributes to a change in the temperature profile of the oceans, meaning that temperatures below the surface are also warmer (32). Storm-induced mixing produces negative feedback as cooler waters are brought to the surface, providing less heat for a storm to feed off of. If the entire temperature profile of the oceans has increased in temperature then this negative feedback is less effective and storms will have a greater potential to build in strength.

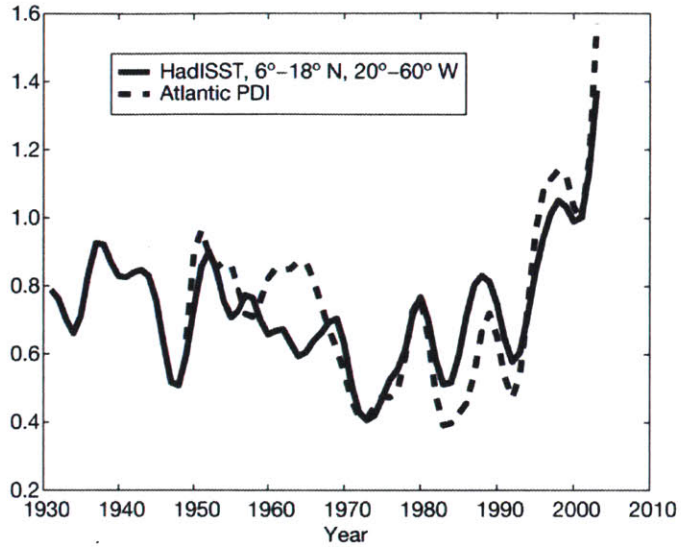

Figure 1-2: A measure of the total power dissipated annually by tropical cyclones in the North Atlantic (the power dissipation index, PDI) compared to September sea surface temperature (SST) (4).

Storm Surge

Storm surges are typically 50 to 100 miles wide and can reach heights as high as 15 feet (1). They are formed by the external forcing of an approaching storm and are known to cause the most damage and deaths during a hurricane. The intensity of a storm is not the only factor governing the magnitude of the storm surge, as discussed below.

We can study how these features influence the magnitude of storm surge using simplified models of the region. The SLOSH model (11), run by the National Hurricane Center, is a hydrodynamic model that applies hurricane simulations with a numerical grid of a coastal region to simulate the resulting storm surge. ADCIRC is a three dimensional finite volume coastal ocean model and is used to model the hydrodynamics around shelves (20). It has a higher resolution than SLOSH and so is computationally more expensive but, integrated vertically it can be used to validate SLOSH results. Due to limited time, we were unable to use ADCIRC for validation in this analysis.

1.3.2 Tides

When a storm makes landfall, the tidal period has an impact on the resulting surge height. Including tides in our assessment adds complications to our analysis. First, a changing sea level has the potential to change the tides in the region as it affects the resonance structure of the tidal systems. The coastal structure, latitude, and bathymetry all add to unique tidal patterns, thus the changes in tides will vary with each location as well. Tides have a nonlinear impact on storm surges, the tidal-surge interaction itself being influenced by shelf geometry. For shallow or more pronounced slopes in ocean floors, the nonlinear impacts of tides on surge heights is more pronounced. Nonlinearity is further pronounced for storm arrivals making landfall at low tide (26).

1.3.3 Subsidence

Subsidence is the phenomenon that describes the sinking of land surfaces, often as an effect of the removal of the Earth's resources. Currently, an estimated 15,000 square miles in the U.S. have been affected by subsidence. The three main contributing factors to subsidence include 'the compaction of aquifer systems, oxidation of organic soils, and the collapse of cavities in carbonate and evaporite rocks' (8). The most severe subsidence since the 1900's has been attributed to the removal of ground water, and some, especially in the Gulf has been a result of the mining of natural gas or oil. As water or these large deposits of fuels are mined from deep wells, the integrity of the support structure is weakened and the land above has the potential to sink or collapse into the newly emptied geological structures. Infrastructure will inevitably be sinking closer to sea level in locations experiencing subsidence, and thus becoming more vulnerable to coastal flooding.

1.3.4 Sea Level Rise

'Three million years ago, during the Pliocene, the average climate was about 2^{o} to 3^{o}C warmer and sea level was 25 to 35 m higher than today's values.'(25) The rate at which ocean levels respond to a 2^{o} to 3^{o}C global warming, however, is still unclear.

The IPCC AR4 cites that 80% of the heat added to the climate since 1961 has been absorbed by the oceans (28). In fact, ocean temperature increases have been recorded as deep as 3000m. This increase in temperature has lead to thermal expansion, contributing to the sea level rise seen thus far since 1900 (3). Figure 1-3 summarizes the anticipated sea level changes from IPCC AR4 based primarily on the changes attributed to thermal expansion.

Table SPM.3. *Projected global average surface warming and sea level rise at the end of the 21st century. {10.5, 10.6, Table 10.7}*

Case	Temperature Change (°C at 2090-2099 relative to 1980-1999)[a]		Sea Level Rise (m at 2090-2099 relative to 1980-1999)
	Best estimate	*Likely* range	Model-based range excluding future rapid dynamical changes in ice flow
Constant Year 2000 concentrations[b]	0.6	0.3 – 0.9	NA
B1 scenario	1.8	1.1 – 2.9	0.18 – 0.38
A1T scenario	2.4	1.4 – 3.8	0.20 – 0.45
B2 scenario	2.4	1.4 – 3.8	0.20 – 0.43
A1B scenario	2.8	1.7 – 4.4	0.21 – 0.48
A2 scenario	3.4	2.0 – 5.4	0.23 – 0.51
A1FI scenario	4.0	2.4 – 6.4	0.26 – 0.59

Table notes:
[a] These estimates are assessed from a hierarchy of models that encompass a simple climate model, several Earth System Models of Intermediate Complexity and a large number of Atmosphere-Ocean General Circulation Models (AOGCMs).
[b] Year 2000 constant composition is derived from AOGCMs only.

Figure 1-3: IPCC emissions scenarios and related estimates of sea level rise

Thermal expansion, however, is only one of four critical factors leading to an increase in sea level. Glacial run-off as well as run-off from the West Antarctic Ice Sheet (WAIS) and Greenland Ice Sheet (GIS) also play a key role in contributing to sea level rise, although the rate and the extent of their impacts is far less understood. The uncertainty from these components has led to a wide range of sea level rise estimates. The estimates used to develop this analysis fall in the range 0.55m and 2m sea level rise by 2100.

Another complication in studying sea level changes is that the changes are not uniform across the globe. Some places on Earth are anticipated to see a greater increase in sea level

than others. This is a result of a number of factors. For one, as glaciers and ice sheets melt, the water contributed to the surrounding ocean is colder than the existing water. An influx of cooler water would therefore diminish the impacts of thermal expansion. Some models predict that the sea level change would not change immediately surrounding the ice sheets but that their contribution to a rising sea level would be felt closer to the equator (21). Also, as glaciers melt the pressure that was once on the land underneath is weakened, therefore, we see land masses rising in some locations as it rebounds from the lack of pressure. This is a slow process that takes centuries to reach equilibrium but is yet another contributing factor to an uneven sea level rise. In fact, some regions, such as the Baltics, have seen a *decrease* in sea level as a result of this phenomenon. Further factors influencing local changes in sea level include surface winds, ocean currents, variations in salinity, and changes in the Earths gravity field (as land ice melts, weight is redistributed across the globe, weakening the local gravitation impacts on water height). (14)

The wide range of estimates described here, and the complexity of sea level distribution, make it difficult to predict a future sea level with any confidence. We anticipate this component of climate change science to evolve rapidly in the coming years.

1.4 Coastal Flood Risk Analysis

In the work that follows, we combine these contributing factors to risk of inundation in a case study to derive a probability distribution of the risk of flooding over the course of this century. Chapter 2 outlines the formulation of our sample case, Galveston Bay. We will discuss the features and vulnerable facilities specific to Galveston Bay as well as the basis for choosing the A1B emissions scenario for our study. We further introduce in Chapter 2 the Atmospheric and Oceanic Global Circulation Models (AOGCMs) used in our analysis. In Chapter 3 we present our analysis. Here, we give a detailed description of the models used for determining the risk of storm intensity, surge, and frequency. We further develop risk profiles for subsidence and sea level rise based on historical data and multiple model predictions. We then present our methodology for combining these risks to make detailed predictions for the vulnerability of coastal infrastructure. Chapter 4 presents our decision

analysis in response to climate change. Here we incorporate a dynamic cost-benefit analysis to optimize the decisions to adapt to the risks of climate change in each decade between 2000 and 2100. Chapter 5 concludes this work with our major findings, policy suggestions, and future work.

Chapter 2

Formulation of a Sample Case: Galveston Bay

2.1 A Decision Focus

A complete analysis of risk to coastal energy infrastructure would need to consider types of infrastructure and different types of damage to it, variation in climate change across locations, various emissions scenarios, and various climate models. We narrow down the scope of this analysis by selecting a sample case, and illustrate, through this case, the methodology in assessing risk so that it can be applied to locations with different conditions. The focus is on provision of information on when and what to do to adapt to the rising risk.

A significant amount of damage to energy infrastructure in recent years has been a result of flooding. We determine that a facility is 'at risk' of damage if it is at risk of being flooded. We compare across climates the probability of a facility being flooded. If a scenario indicates that water level has reached the facility, through the combined effects of our physical risk factors, then we consider the facility flooded. We report our results as an annual probability of flooding and use these estimates in the decision making framework in Chapter 4.

With increasing threats of climate change, response decisions are needed for infrastructure in harm's way. We consider there to be three types of responses here. The first is to continue with business as usual and to face the increasing risks of damage. The second is to

abandon a facility. If the expected costs of damage are so high that they offset the benefit of running the facility, then abandoning the facility may be the least costly option. And third, is the option to build protective levees. With this last option, the decision options continue to include the optimal height and length of the levees and the best time to construct the levees or to add extra height to the levees. Of course other options include a combination of these three. For example, business as usual at first and then either abandonment or adaptation.

2.2 Choice of Sample Set of Facilities

Galveston Bay While the U.S. coastline is home to a wealth of energy facilities (see Figures 1-1), Galveston Bay is home to some of the most vulnerable energy infrastructure along the coastline (see Figure 2-1). We chose to focus our analysis on the infrastructure in Galveston due to a number of key features specific to that region.

Historically, Galveston Bay has seen incredibly destructive hurricanes. The Galveston Hurricane of 1900 is still to this day the deadliest storm to have hit the United States, killing upwards of 6000 people. Following the Hurricane of 1900, Galveston underwent extensive reconstruction as most of the buildings were left damaged, if not destroyed. A retaining sea wall, 17 feet tall and originally 3 miles long, was built by 1910 in time to blunt the fourth most destructive storm in the 20th century, which made landfall in Galveston in 1915 (24). The sea wall was further a useful addition during the category 4 hurricane that hit Galveston in 1932, the storm surge from the Category 4 hurricane that landed in Freeport, TX, and Hurricane Alicia in 1983 which was the costliest hurricane seen within that decade (16). Major reconstruction of the town has taken place to raise homes several feet in anticipation of new storm arrivals. Despite this, Hurricane Ike still caused nearly $30 billion in damage to the city in 2008.

The Gulf Coast in general has a history of incredible storm damage, with nearly half of the most destructive storms of the 20th century in the U.S. blowing through the Gulf. Coastal communities, including Galveston, have begun adapting with sea walls and levee

systems, but today Galveston and Houston are still considered to be highly vulnerable regions to intense tropical storms (24).

Aside from being historically disaster prone, there is a significant number of critical energy facilities operating in Galveston Bay. It is an active oil seaport, so has become a location populated with large oil refineries as well as the Big Hill Strategic Petroleum Reserve. Aside from oil, a number of natural gas and coal power plants are in operation in Galveston. Texas produces more energy than any other U.S. state, accounting for over 30% of United States natural gas production and over 20% of the crude oil production (29). Much of this production depends of the facilities in Galveston Bay.

Another unique feature of the region is the topography, and the changing topography of Galveston. The region is low lying, with much of it's infrastructure sitting within 15 feet of mean sea level. Apart from being relatively close to sea level, Galveston is also experiencing some of the most severe subsidence in the U.S. (8); some regions have sunk as much as 10 feet since 1906 (see Figure 2-2). Much of the land subsidence can be attributed to the removal of ground-water, but other contributing factors exist include the mining and drilling for oil and natural gas (8). All of these factors combined add to relatively vulnerable energy infrastructure as well as a changing vulnerability as subsidence continues, ideal for our analysis.

Three Facilities We refine our analysis further by selecting three high-capacity, low-lying facilities to focus on for our risk assessment. These include the Texas City Oil Refinery (elevation 5, 6, 8 feet above mean sea level with 199,500, 76,000 and 467,720 barrel capacity respectively), the Big Hill Strategic Petroleum Reserve (elevation of 11 feet, 160 million barrel capacity), and Baytown Energy Center LP (5 feet elevation, 915 MW Gas-fired combined cycle). We focus our analysis on these three facilities to analyze the change in risk of them being flooded over ten years.

2.3 Scenarios of Greenhouse Gas Emissions

Research indicates that the severity of anthropogenic climate change is dependent on greenhouse gas emissions rates (27). Therefore, the potential for flooding in 2100 will be affected by the rate of emissions over the course of this century. Studying many emissions scenarios was beyond the scope of this project, we therefore choose to study the impacts from just one scenario, the A1B emissions scenario as defined by the IPCC AR4. The A1 family of emissions scenarios describe a future with rapid economic growth, population peaking mid-century, and a rapid introduction of new technologies (28). Under A1B, energy is derived from a mix of fossil-fuel and non-fossil fuel sources. Figure 2-3 shows the IPCC emissions trajectories and Figure 2-4 shows the projected temperature increase for these emissions scenarios. Models predict that under the A1B scenario, temperature change by the end of this century will be somewhere between 1.7 and 4.4 ^{o}C, with the best estimate being 2.8^{o}C and a sea level rise between 0.21 and 0.48m relative to the temperature and levels from 1980-1999. This temperature change will result in a change in hurricane activity as well as a change in the rate of sea level rise.

2.4 Atmospheric-Ocean General Circulation Models (AOGCMs)

AOGCMs are used to study how the climate will react to the A1B emissions scenario. Analysis in the IPCC AR4 is based on the projections of 18 AOGCMs, we work with four of the 18 for the hurricane arrivals (Table 2.1) and six for sea level rise (Table 2.2). See Figure 2-4 for the projected range of climate responses that the AOGCMs predict for various emissions scenarios. A1B is displayed in Figure 2-4 to be a compromise between high and low emission scenarios and is predicted to produce a range of temperature increases centered roughly around 3^{o}C.

Table 2.1: Global Circulation Models from IPCC AR4. Temperature projections are based on the A1B emissions scenario.

model name	Institution	predicted temperature increase by 2100
CNRM-CM3	Le Centre National de Recherches Meteorologiges, Meteo-France	2.9^{o}C
ECHAM	Max Planck Institution	3.4^o
GFDL-CM2.0	NOAA Geophysical Fluid Dynamics Laboratory	2.7^o
MIROC 3.2	CCSR/NIES/FRCGC, Japan	4.5^o

Table 2.2: Global Circulation Model's from IPCC AR4. Temperature and sea level rise estimates based on A1B emissions scenario.

model name	temperature change	sea level rise
ccma cgcm 3.1	2.6005 ^{o}C	0.2102 m
giss aom	1.7929 ^{o}C	0.3433 m
giss model e r	1.7485 ^{o}C	0.2808 m
inmcm 3.0	2.1573^{o}C	0.2385 m
miroc 3.2 (high res)	3.7111 ^{o}C	0.3375 m
miroc 3.2 (med res)	3.1049^{o}C	0.2757 m
mri cgcm- 2 3.2a	2.0652^{o}C	0.1338 m

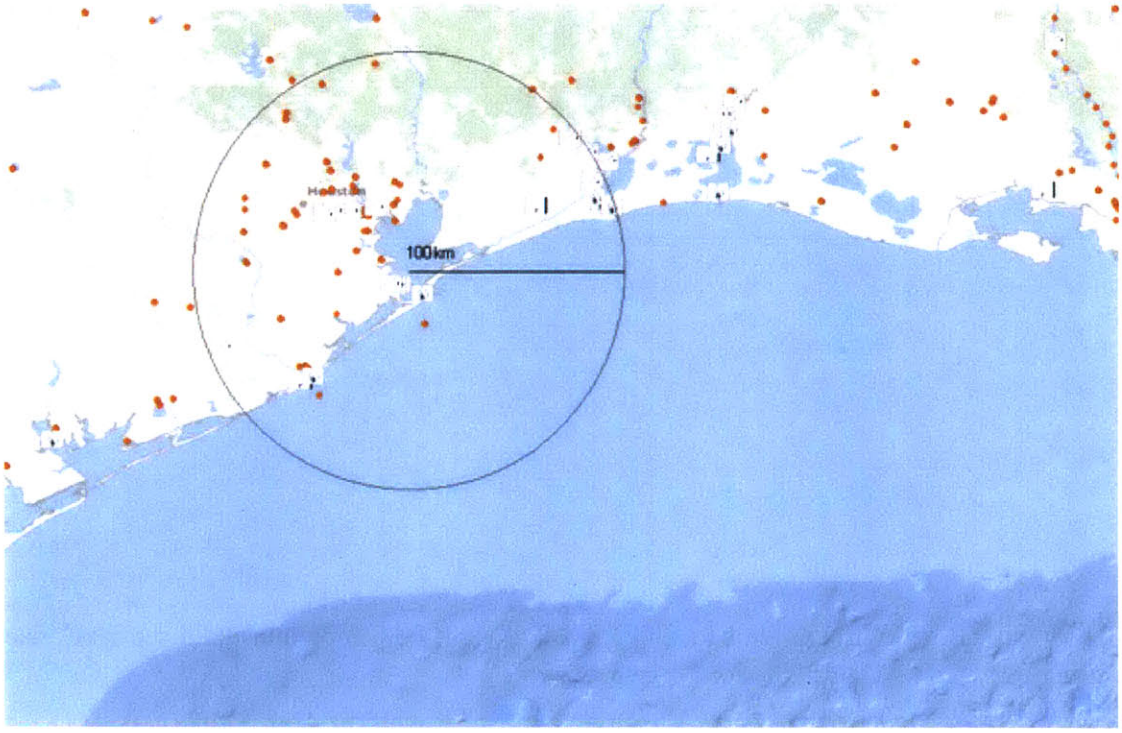

Figure 2-1: Energy infrastructure in Galveston and surrounding regions

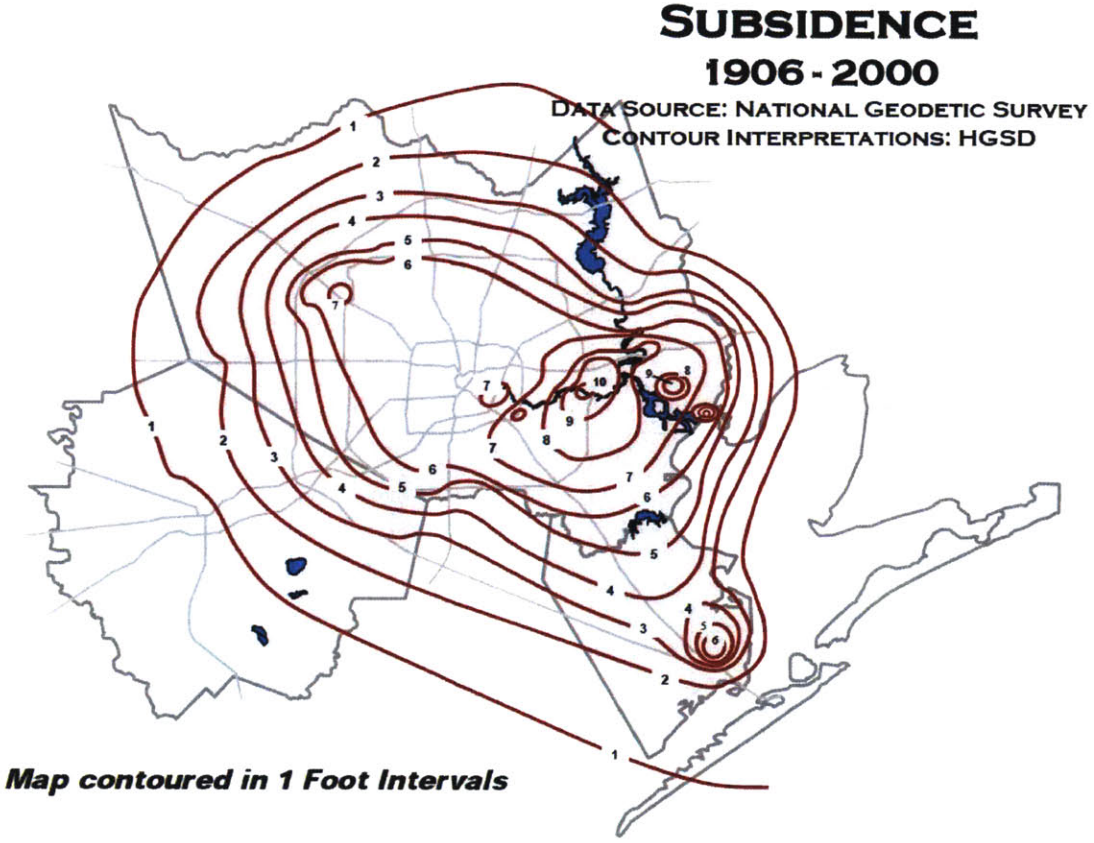

Figure 2-2: Land subsidence in Texas

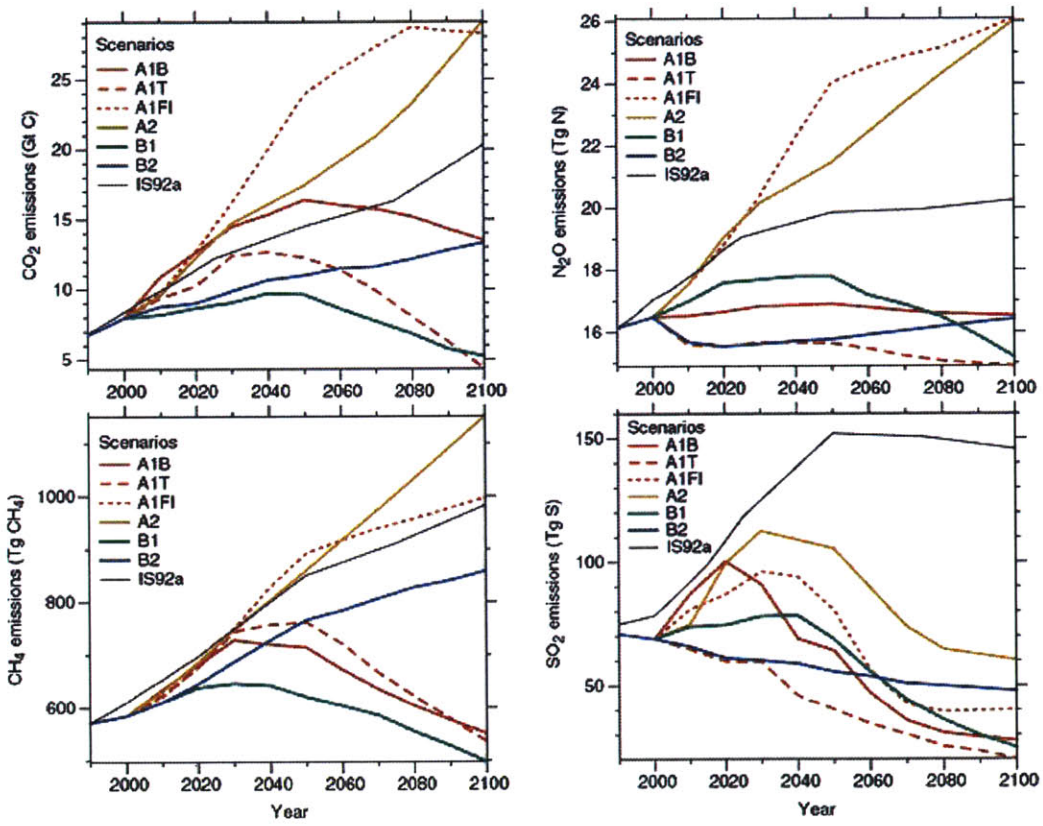

Figure 2-3: IPCC AR4 emissions scenarios

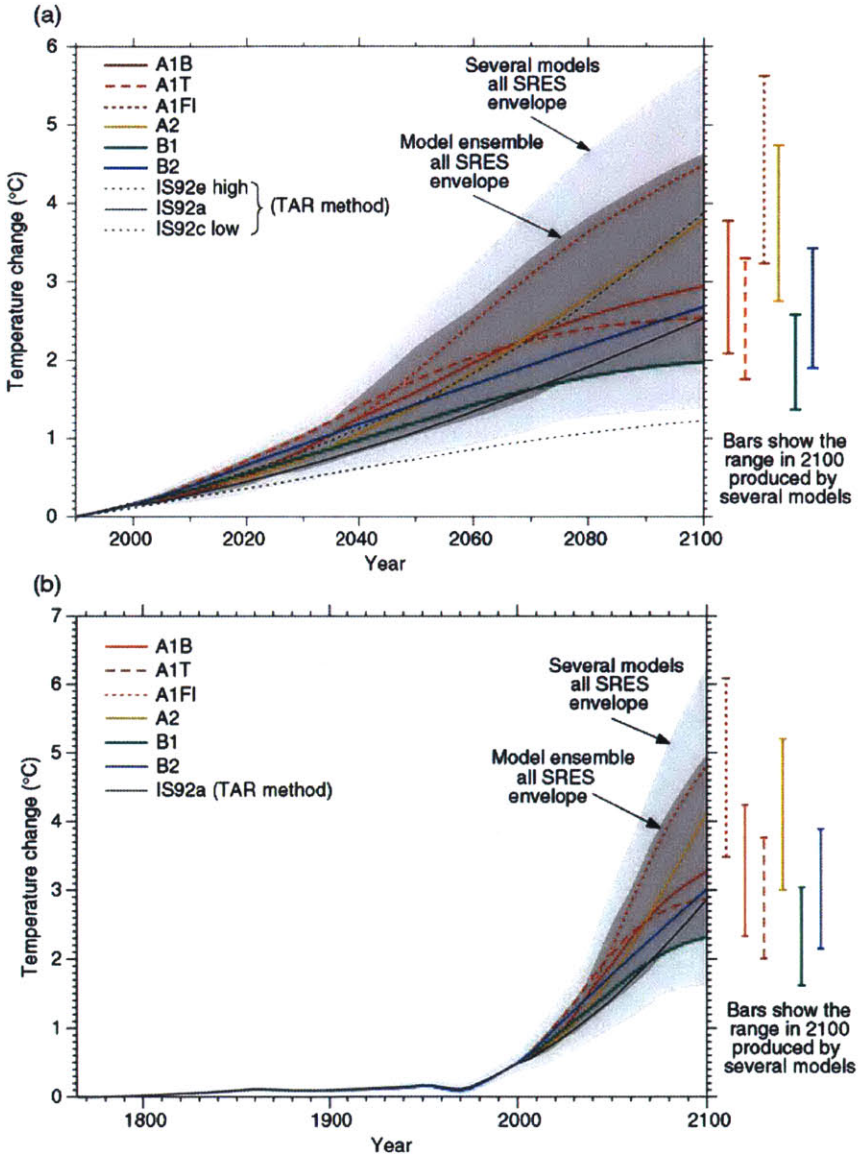

Figure 2-4: Simple model results from the IPCC AR4: (a) global mean temperature projections for the six illustrative SRES scenarios and (b) Same as (a) but results using estimated historical anthropogenic forcing are also used.(28)

Chapter 3

Physical Risk to Galveston Bay Facilities

3.1 Risk Components

For our sample case, we conduct a risk analysis to determine how the risk of flooding changes between a climate in 1980-2000 and a climate in 2080-2100. For simplification, throughout the rest of the analysis, we occasionally refer to these two decade-long periods as 2000 and 2100 respectively. We study the change in risk by looking specifically at these two separate time frames and using AOGCMs as well as numerical approximations to predict how this risk is changing over time. Recall that the future scenario is conditional on an A1B emissions trajectory and that the climate models used in this study operate under this assumption. To consider the full risk, we first break down the analysis into probability distributions of each contributing factor in each projected climate.

3.1.1 Storm Intensity and Surge[1]

Storm Intensity

We begin by looking at tropical cyclone intensity in both climates. Since there is a relatively limited record of hurricane activity due to their infrequency, it is difficult to base our current climate's trends strictly on historical data. For this reason, a method developed by Emanuel is used to generate a large number of sample storms to produce probability

[1] Special thanks to Dr. Ning Lin who performed runs of models used in the analysis.

distributions of storm intensities that are "statistically robust estimates of the probability distributions of storms in different climates" (5). Synthetic hurricanes are simulated under conditions projected by large scale Global Circulation Models (GCMs) to see how changes in environmental factors can alter hurricane activity. The GCMs used for this analysis are from the IPCC AR4 and are described in Table 2-1. They include CNRM, ECHAM, GFDL, and MIROC, each run under the A1B emissions trajectory.

GCMs are numerical models representing earth's physical processes that govern the atmosphere, ocean, and cryosphere interactions. The models used in the IPCC AR4 typically have between a 250km and 600km horizontal resolution with 10 to 20 vertical layers (IPCC AR4 Data Distribution Centre). The GCM's themselves are too coarse to be used in the modelling of tropical cyclone activity so a more resolved model is embedded into the GCM's to capture the effects governing tropical cyclone activity.

Emanuel's method for tropical cyclone generation performed involves three steps;

1. *Genesis by Random Seeding.* This synthetic seeding technique draws 'storm seeds' randomly distributed through space and time. These seeds are initiated as warm-core vertices with peak winds of $12ms^{-1}$ with nearly no midlevel humidity. They tend to quickly decay due to their small potential intensity, vertical wind sheer, or low midtroposheric entropy.

2. *Tracks.* A "beta and advection" model creates tracks from these seeds based on vertically averaged wind-sheer and then corrected for beta shift. The wind sheer is generated using synthetic wind Fourier time series of 850 and 250 hPa. These two scalar wind fields statistically conform to the same monthly mean, variance, and co-variance as wind statistics from present climate data from the National Centers for Environmental Predication-National Center for Atmospheric Research reanalysis dataset. Tracks are generated from these wind fields with generous geographic boundaries, allowing them to continue to far greater latitudes and longitudes than is typically seen. For our research, we specify a location (Galveston, 29.3^o N, 94.5^o W) and a filter with a radius of 100 km (see Figure 2-2). Only tracks that pass through the filter are kept, the rest are discarded. This allows for us to include tracks seeded any-

where in the Atlantic to be included in our analysis, provided that the track passes through the filter. Figure 3-1 illustrates a set of storm tracks that are kept for our analysis.

3. *Intensity.* For the tracks that pass through the filter, the Coupled Hurricane Intensity Prediction System (CHIPS) is run to determine the intensity of the storm. The wind shear used in CHIPS is the same wind field used for generating the tracks, therefore creating consistent storm motion and wind shear. Generally the storms dissipate well before the end of their tracks.

Only tracks exceeding a minimum windspeed of 34 mph within our specified filter are kept. The model continues to generate seeds until N_{tracks} storm tracks have been generated that both exceed the minimum intensity threshold and pass through the filter. N_{tracks} is set to equal 3000 for each model and N_{seeds} is the number of seeds required for a given model to generate 3000 storm tracks. N_{seeds} will therefore differ among models.

This method is used to generate hurricanes off of GCMs under 1980-2000 conditions, and then is run again under the A1B emissions trajectory to reach a new climate for 2080-2100. The data input for both of these runs was obtained mostly from the World Climate Research Program (WCRP) third Climate Model Intercomparison Project (CMIP3) multi-model dataset. We draw conclusions about the change in intensity of storms across climates by comparing the distribution of storm intensities generated through these models. We first look at the atmospheric storm conditions along a tropical cyclone's track before determining the resulting storm surge.

The output of each storm track provides us with information on a 2-hour time step. This information includes

- storm location
- radius of maximum wind
- maximum windspeed
- pressure

We initially compare maximum windspeed from each storm and model across time. For every hurricane track, we choose the location along the track closest to our specified point and note the maximum wind speed generated at that point in the track. Figure 3-2 illustrates the difference between the models' cumulative probability distributions of windspeed conditional on a storm arriving. Figure 3-3 indicates the difference between climates within the GFDL model. (Not shown are our results that indicate that the GFDL GCM produces the largest increase in average storm intensity.) NOAA uses GFDL for the North American Regional Climate Change Assessment Program. Although in our analysis we consider the results from all models, we focus on GFDL in the illustration of our results.

3.1.2 Surge Simulations

As hurricane intensities increase, there is a general anticipated trend of increased storm surges, leading to a greater potential for flooding.

Storm surges occur when sustained wind forces act on a body of water, forcing water up onto the shore. The height of the storm surge is determined by a number of factors:

- the bathymetry around the coastline
- the size of the storm
- the speed of the wind
- the direction of the wind
- the time of the tidal cycle
- the speed and direction in which the storm is approaching

A further feature of a storm surge is that it creates a sloping ocean surface, resulting in more extreme surges in the upper reaches of bays (32). Due to all of these factors, it is difficult to make a straight forward calculation relating windspeed to storm surge. There are attempts to generalize the relationship between wind velocity and storm surge such as the relationship described by the Saffir-Simpson scale, however, these relationships are too crude for the purposes of our analysis (12). Instead the SLOSH model (Sea, Lake and

Overland Surges from Hurricane) was used. It applies forcings from each hurricane run to a finite coastal ocean model of Galveston's surrounding coastline to generate corresponding maximum surge heights.

The storm surge heights that are used in this analysis involve the maximum surge height for three different locations in Galveston for every storm. Surge heights from three different locations were recorded in order to get a broader geographic representation of maximum surge height. The three points that were used include Point A located at 29^o3 N and 94^o5W, Point B located at 29^o7 N and 94^o2W, and Point C located at 29^o2 N and 94^o2W.

Figure 3-4 shows that while there is some variation across locations in surge heights, it isn't terribly dramatic. For this reason we refer to the results from Point A for the remainder of our analysis, which is the closest point to our facility of interest.

We compare the differences in surge heights across climates in Figure 3-5 by contrasting the probability density functions in 2000 against 2100 in the GFDL GCM. These results indicate the change in distribution of surge height assuming there is no sea level rise.

3.1.3 Annual Frequency and Hurricane Arrival Processes

As disturbances are seeded in the models during genesis, a number of conditions must exist for the seeds to develop into tropical storms. As described in Chapter 1, hurricanes require pre-existing weather disturbances, atmospheric moisture, warm ocean water, and light prevailing winds. The capacity to which these ideal conditions are met change with a warming climate and a different potential is reached for these seeds to develop into storms. As discussed, each climate model and time period produces a different distribution of storm intensities. Being able to use these distributions to anticipate storm arrivals in a given year requires each climate model to be calibrated. This calibration is done using a single constant, based on the hurricane database (HURDAT) record (10), to achieve an annual frequency. HURDAT is a 'best track' dataset that was updated in 2001 and again in 2002 to include reanalysis data for storm tracks as far back as 1851. The annual frequency for the 1980-2000 period in our analysis in Galveston Bay is taken from HURDAT and is the

observed number of tropical storms, above a specified minimum threshold of 34 mph, that pass through our filter in a year.

Initially in the analysis, the models are calibrated to the observed number of *genesis* events in a year (i.e. actual number of seeds) averaged between 1981 and 2000. Let i be the specific AOGCM and α be the observed annual genesis frequency (seeds/year), which is assumed constant over time. Each model's calculated annual frequency of *storm* events, AF_i^c, can then be stated as

$$AF^c_{i,2000} = \alpha \times \frac{N_{tracks}}{N_{seeds,i,2000}}, \tag{3.1}$$

The analogous equation holds for 2100. This procedure for computing $AF_{i,2000}$ and $AF_{i,2100}$ is internal to the model. This, however, produces different $AF_{i,2000}$ values for each model because a different $N_{seeds,i,2000}$ is required for each model to produce $N_{track} = 3000$. It is expected that there are biases within each model so an additional calibration is performed by setting annual frequencies for each model under the current climate, $AF_{i,2000}$, to 0.26, the observed present day annual frequency at Galveston based on HURDAT. The correction for 2000 is then

$$AF_{i,2000} = AF^c_{i,2000} \times K_i = 0.26 \tag{3.2}$$

$$K_i = \frac{0.26}{AF_{i,2000}} \tag{3.3}$$

K_i is used to calibrate model i's future annual frequency, which is denoted as $AF^c_{i,2100}$;

$$AF_{i,2100} = K_i \times AF^c_{i,2100} \tag{3.4}$$

or

$$AF_{i,2100} = K_i \times \alpha \times \frac{N_{track}}{N_{seeds,i,2100}} \tag{3.5}$$

Without this calibration, we would only see the proportional increase in storms within a model and not the actual anticipated frequency. The calibrated annual frequencies are listed in Table 3.1.

Hurricane Arrival Process. We assume that hurricane arrival times are independent of one another and therefore follow a poisson distribution with annual frequency as the parameter. Given AF_i, we can calculate the probability of k storms occurring in one year;

$$P(k|AF_i)_i = \frac{AF_i^k e^{-AF_i}}{k!} \tag{3.6}$$

The probability distributions thus far show the risk of flooding given a storm arrival. We seek, however, to find the distribution of the *annual* risk of flooding instead. To do this, we use a numerical approximation to derive the resulting distribution from the poisson arrival process with annual frequency, AF_i, as the poisson parameter . Since this is a poisson process, more than one storm could arrive in a given year. Define N_k as the number of storm arrivals in one year. Of these arrivals, we only keep the highest resulting surge for our distribution since any lower surge height will be surpassed by the highest surge in that year. For this approximation, we sample 100,000 times by first sampling the number of storms, N_k, from a poisson distribution, then drawing N_k times from the distribution of storm surges given an arrival. We record the highest of the N_k storms for our yearly arrival height. The result is a new distribution of the annual probability of surge heights. Figure 3-6 illustrates the resulting annual storm surge height distribution in red and contrasts this distribution to the storm surge probability distribution given a storm arrival, which is indicated in blue. For the remainder of the analysis, we use the annual surge height probability distribution (red curve). One very notable difference between these two distributions is that there will be a high probability of no storm arrivals in a year. The probability of this occurring is simply;

$$P(k = 0, AF_i)_i = e^{-AF_i}. \tag{3.7}$$

Tidal Effects

Tides in Galveston don't have a significant impact in this study as they only vary by about a foot from mean sea level. If this analysis is to be applied to regions with a greater tidal fluctuation then more attention should be paid to the incorporation of tides into models. For

our analysis, we randomly select a tidal height from a sinusoidal distribution with amplitude 1 foot and add it linearly to the surge height. Note that, despite the sinusoidal function being less than accurate, this is further an inaccurate depiction of reality since storm surges occur over a period of time allowing tidal heights to fluctuate within that time.

3.2 Sea Level Rise

We model the addition of sea level using two analytical components. There is s stronger scientific basis for estimating sea level rise resulting from thermal expansion. This is one component of our analysis. The great ice sheets are still lacking sound scientific evidence and reasoning for how they will melt. We isolate this component from thermal expansion so that it can be easily modified as the science evolves.

3.2.1 A. Thermal Expansion

Since some of the models in the IPCC AR4 include thermal expansion in their output, we run our analysis off of these predictions, however, the four climate models used to study hurricane arrivals do not all include a sea level component, although they do include temperature change. We therefore derive a relationship between temperature and sea level rise using six GCMs from the IPCC AR4 that do include sea level output in their forecasts. These models are listed in Table 2.2 and their temperature projections and sea level rise projections are shown in Figures 3-7 and 3-8.

From the results in Table 2.2, we run a regression (see Figure 3-9) and derive a crude estimate of a relationship between temperature change and sea level rise for each of these models. Some literature suggests that the relationship between thermal expansion and atmospheric temperature linear, especially in the near-future (14) and I use this assumption in the regression. This estimate is based on the decade averaged change in temperature between 2000 and 2100 and the decade averaged change in sea level between 2000 and 2100. The temperature change pathway is not included in the regression, I assume the resulting change that is projected at the end of the century to be sufficient. I further assume

the residuals from the regression to be normally distributed.

From this regression, we conclude that the risk of thermal expansion follows a normal distribution with mean of $0.027T_i + 0.19$, and variance of 0.17367^2, where T_i i the decade average temperature change across the century.

We sample from this distribution, where T_i is the corresponding temperature of the models used for hurricane analysis, and linearly add the sea level rise contributions to the corresponding surge heights. We lose some accuracy in assuming a linear addition; as the ocean level rises, the shape of the coast line and the coastal bathymetry changes and has the potential to alter the resonance of the system. This ultimately affects the ways that waves move onto shore meaning that storm surges could be amplified or diminished with an additional sea level rise. However, we don't expect that an increase of 1-2m would alter the system enough to observe a change much different from a linear addition. Therefore, we accept this to be a rough approximation.

B. WAIS and GIS

The massive uncertainties in the contributions to sea level rise from the great ice sheets make it difficult to incorporate into our risk assessment with confidence. But to ignore this component of the risk is misleading as it could potentially contribute an additional meter or more of sea level. Scenario analysis has been one approach in previous methods. Instead, we've chosen to estimate uncertainty distributions for sea level rise and add this linearly to our flood height estimates from the previous parts of this analysis.

Please note that expert elicitation is needed but missing in our analysis to date. Recent studies have shown a wide range of sea level rise scenarios. Kastman et al. , anticipates a 'high level' scenario of 0.55 to 1.15 m in global mean sea level rise by 2100 (15). Nicholls et al. predicts that with a 4^oC temperature increase, sea level could increase by as much as 2m although an undefined but low probability is attached to the high end of this range (22). Vermeer and Rahmstorf predict a rise in sea level between .97 and 1.56m above 1990 levels by 2100 with a model average of 1.24m (30), and Nordhaus' RICE model anticipates that with a no policy scenario, (emission trajectory similar to A1B) that we will see a sea level

rise of 0.727m by 2100.

Some studies of coastal risk add a scenario value of the WAIS and GIS effects to other coastal risk (e.g. Ning et al. 2012) which gives an impression of the total risk. However, to support the decision analysis framework developed here, an expression of the uncertainty in this effect is needed. (Adding a scenario value involves the implicit assumption that the ice sheet contribution is certain at the scenario value applied.) To facilitate the decision making process, we create a risk distribution to reflect the studies completed to date. We use a log normal distribution with mean 0.6m, and standard deviation of 0.14m (Figure 3-10). We use a lognormal so that the results are positive sea level additions and so the extremes can be captured in the tails.

Subsidence

We approach this portion of our analysis, again, with wide uncertainty. The rate of subsidence will depend on a few factors, namely what we draw from the ground (water, natural gas, oil). So the rate at which subsidence occurs can be altered as changes in policy and human activity occur. There is also possibility of technology advancement that could slow down subsidence. Given these unknown factors, predicting the rate of subsidence is a challenge. We run our analysis off of a distribution based roughly on the previous century's subsidence levels. The locations of our interest sit in a zone that has seen roughly between 3 and 4 feet of subsidence between 1906 and 2000. To estimate this coming century's subsidence, we use a triangular distribution. We assume that there will likely be a slower rate of subsidence given an increased understanding of the causes. We therefore assume a mean of 2 feet and use 4 feet as our upper bound. We use zero for our lower bound and construct a triangular distribution on these three parameters. (see Figure 3-11) With clearer policies and with appropriate models, we would derive a more realistic distribution. We use a triangular distribution to bring attention to the lack of understanding behind the extent and risks of subsidence.

Table 3.1: Calibrated annual frequencies in Galveston using the current annual frequency of 0.26.

model	AF in 2000 ($AF^c_{i,2000}$)	AF in 2100 ($AF^c_{i,2100}$)	K_i	AF in 2100, calibrated ($AF_{i,2100}$)
echam	0.3669	0.3902	0.7086	0.2765
gfdl	0.3613	0.8430	0.7196	0.6066
miroc	0.1929	0.2124	1.3478	0.2863
cnrm	0.3729	0.4077	0.6972	0.2843

3.2.2 Combining components into a physical risk measure

To account for all of these risks occurring, we combine these many distributions under each climate scenario. For the present scenario, sea level rise and subsidence are ignored and only storm arrivals under current intensities and frequencies, and tides are considered. To accomplish amalgamating the distributions, we use a numerical approximation by sequentially sampling from each of the distributions, and adding the sampled sea heights or sunken ground levels together. We repeat this sampling method (i.e. Monte Carlo method) for each climate 10,000 times to get an approximation of the combined risk distributions for each climate. The change in risk distribution across climates is shown in Figure 3-12. For the GFDL model and under our assumptions of sea level rise and subsidence, the analysis concludes that for a facility sitting at 5 feet, under 2000 climate conditions, there is a 1.27% chance of flooding in one year. This probability increases to 47.16% in the 2100 time period under A1B. See Table 3.2 for the results from all four models.

3.3 Tables and Plots

Table 3.2: Probability of Flooding for facility at 5 feet in elevation

model name	Annual Flood Risk (1980-2000)	Annual Flood Risk (2080-2100)
CNRM-CM3	0.0095	0.3886
ECHAM	0.0089	0.3871
GFDL-CM2.0	0.0127	0.4716
MIROC 3.2	0.0108	0.3973

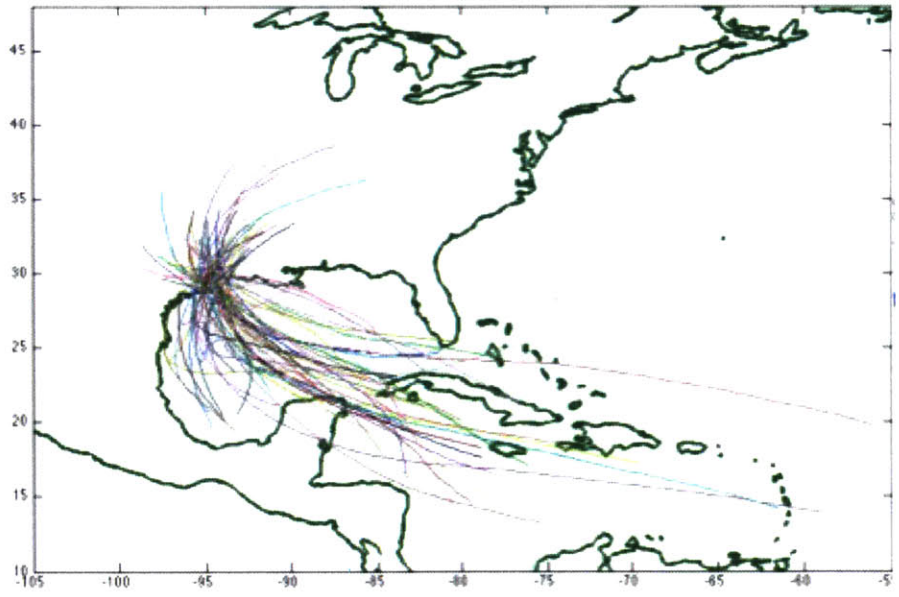

Figure 3-1: 50 of the storm tracks used in our analysis, passing through filter centered at Galveston (see Figure 3-1).

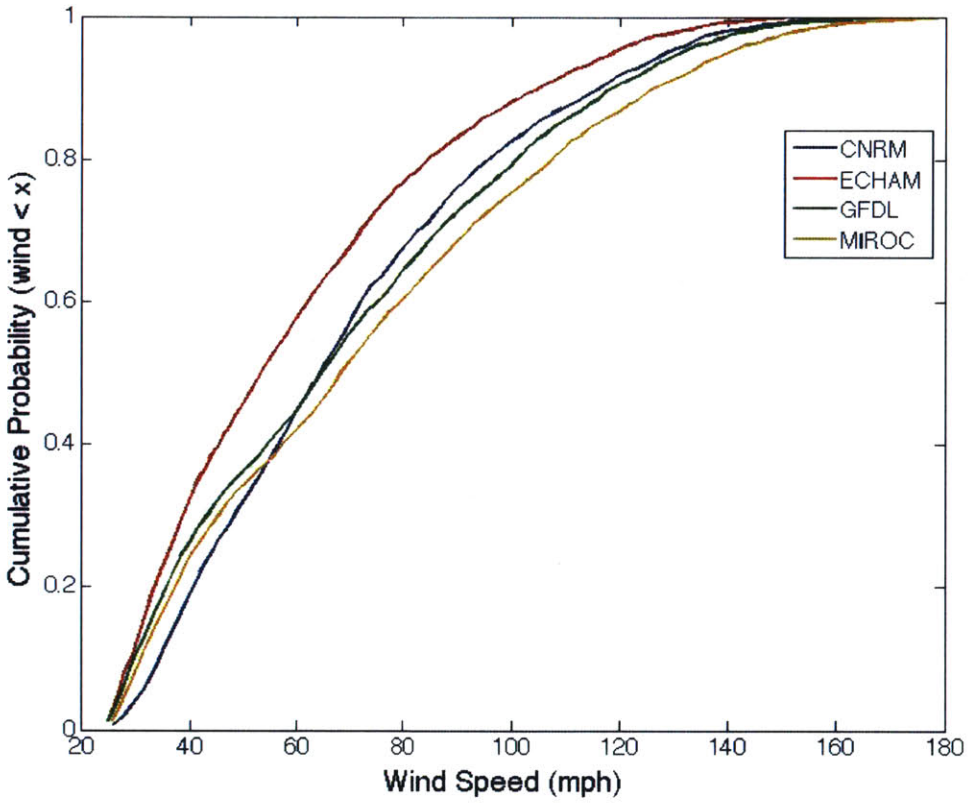

Figure 3-2: Maximum wind speed cumulative distribution, conditional on storm arrival in Galveston Bay, 2000

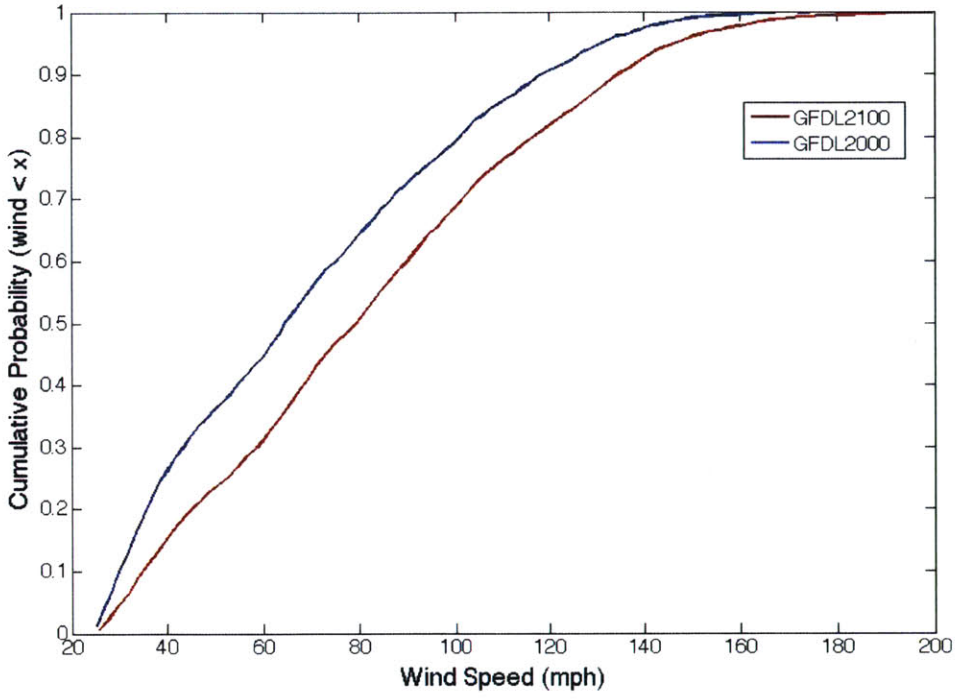

Figure 3-3: Cumulative distribution of windspeeds in Galveston Bay for the GFDL GCM, 2000 and 2100 conditional on storm arrival

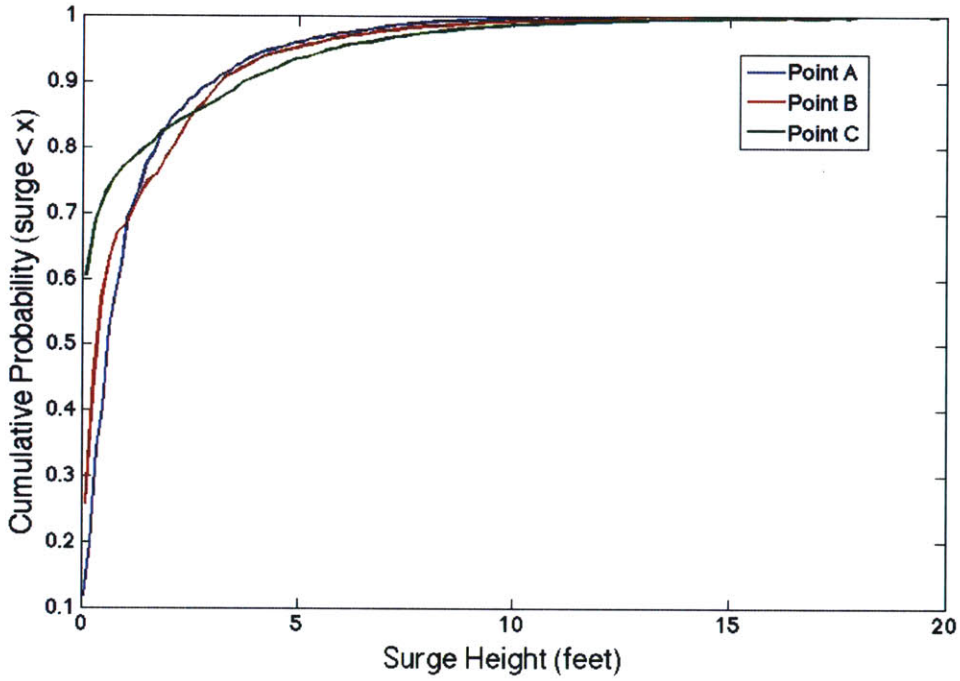

Figure 3-4: Cumulative distribution of surge heights across three locations in Galveston Bay, 2100

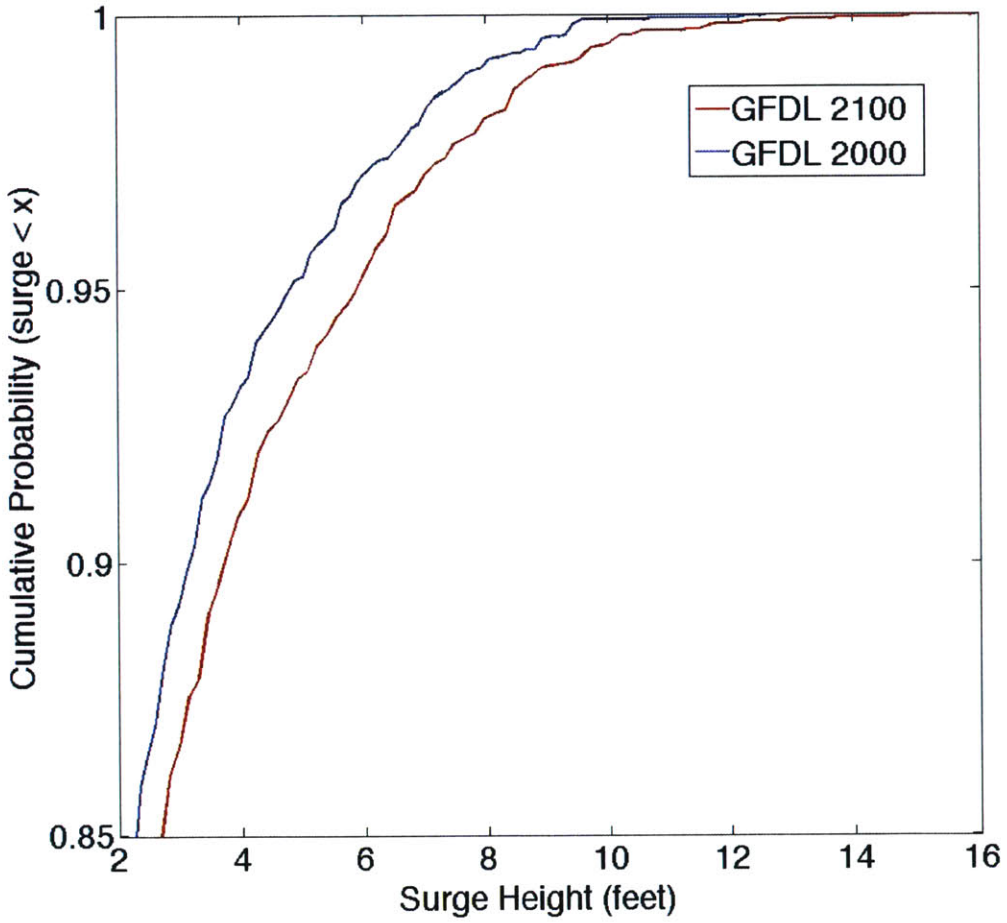

Figure 3-5: Cumulative distribution of surge heights in Gavleston Bay, 2000 and 2100 for the GFDL GCM

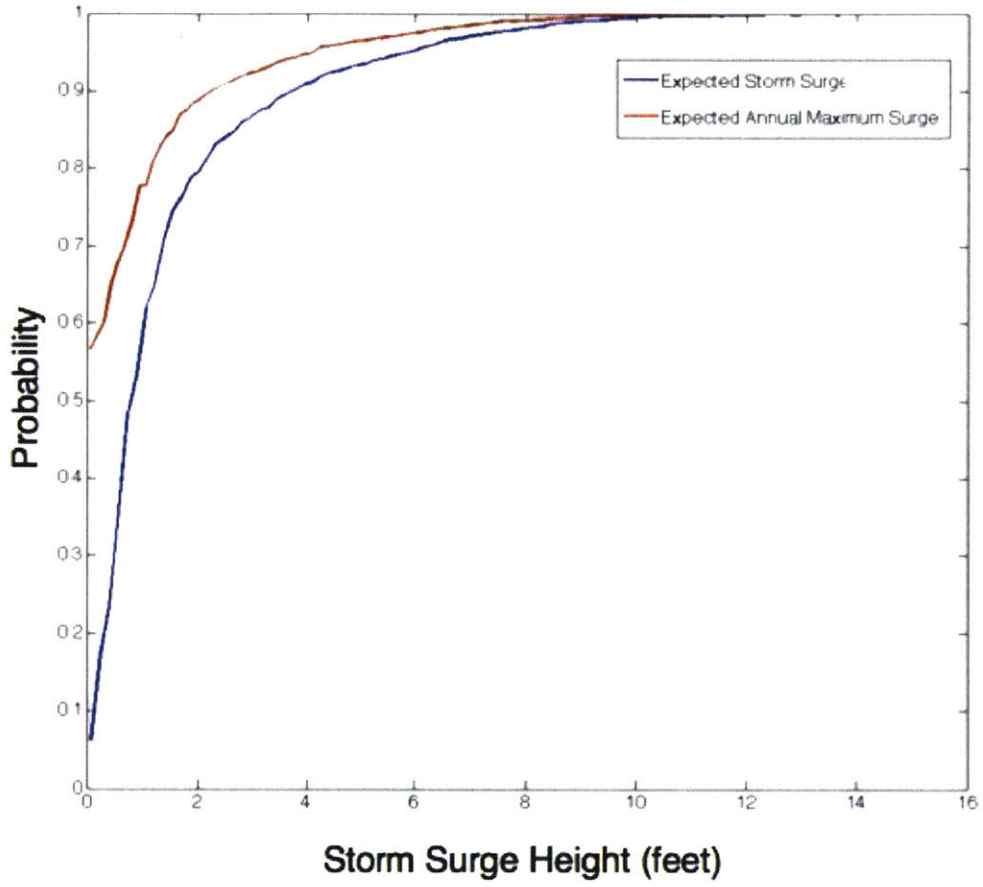

Figure 3-6: Cumulative Distribution of the expected storm surge in Galveston Bay given the arrival of a storm (blue curve) against the expected maximum surge height in a given year (red curve), for the GFDL GCM

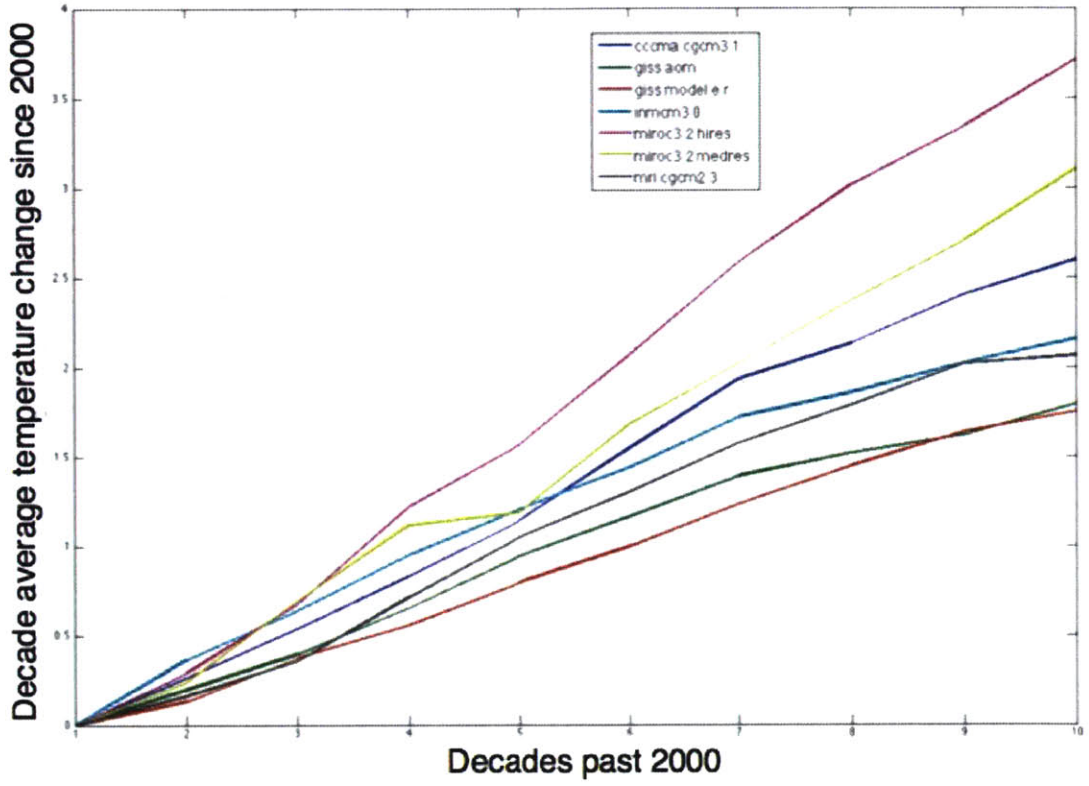

Figure 3-7: Decade averaged temperature projections from IPCC AR4 under the A1b emissions scenario

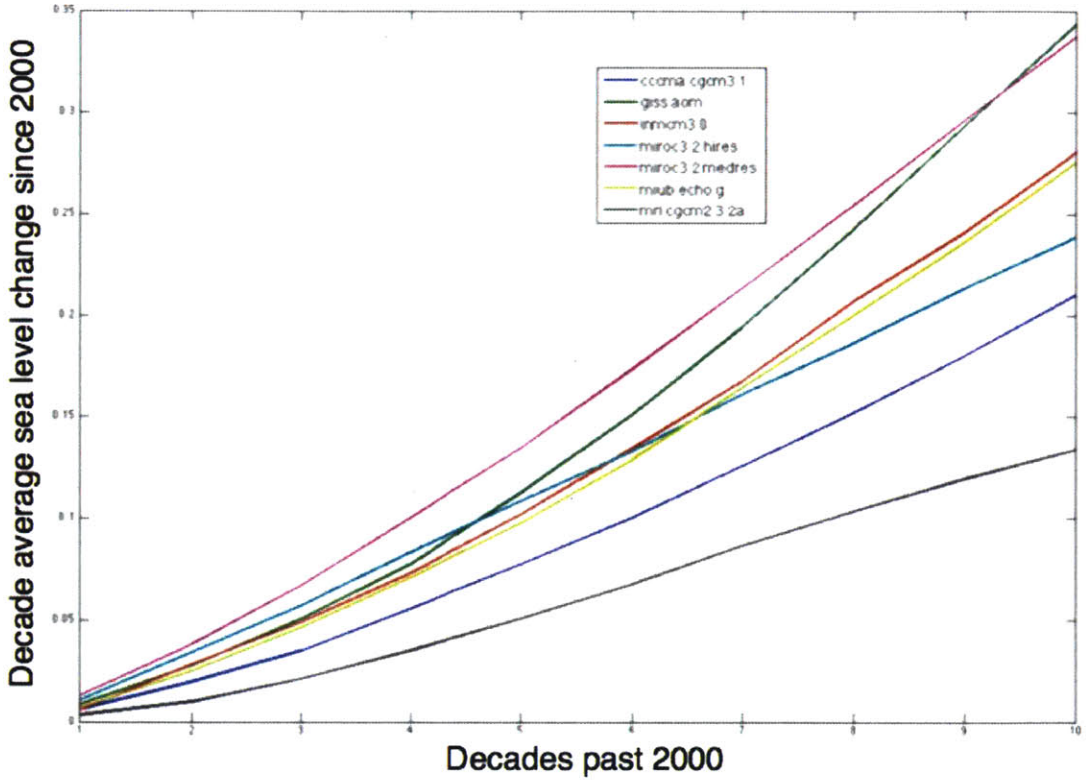

Figure 3-8: Decade averaged sea level rise projections from the IPCC AR4 under the A1b emissions scenario

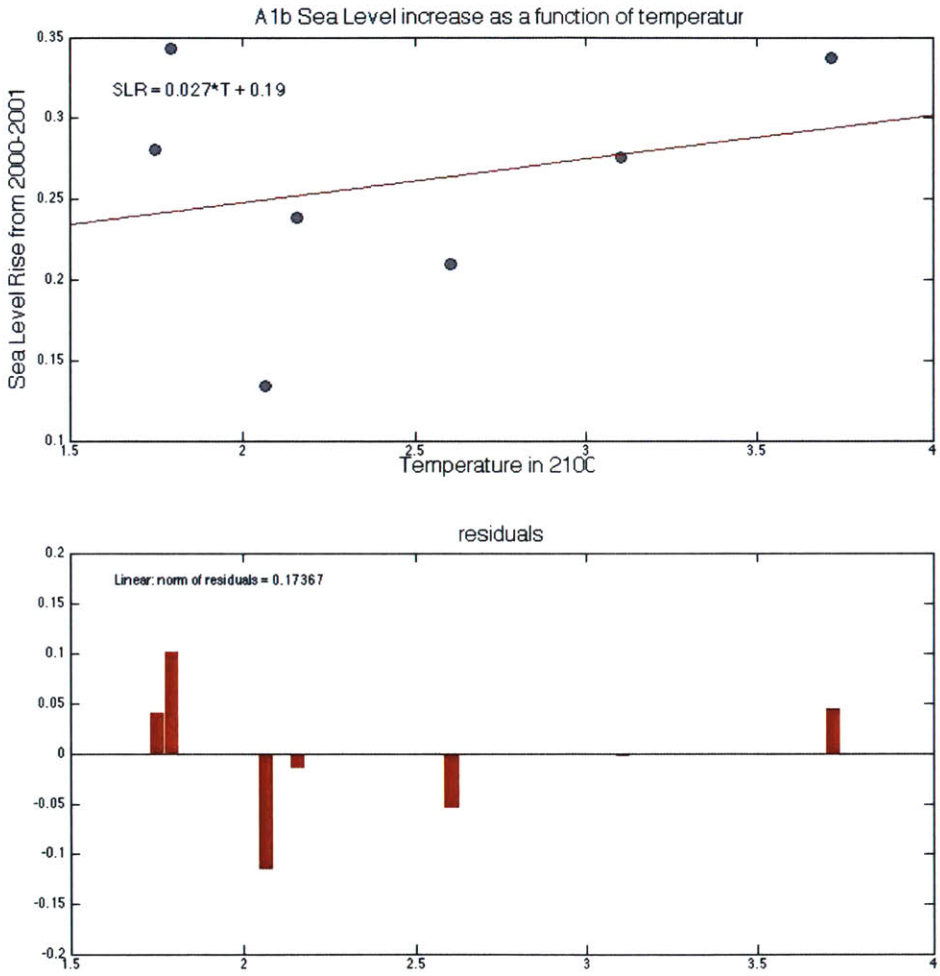

Figure 3-9: Linear regression of decade averaged 2100 temperature projections (Figure 3-8) vs 2100 sea level rise projections (Figure 3-9), from the six models from Table 2.2 run off of A1B emissions scenario.

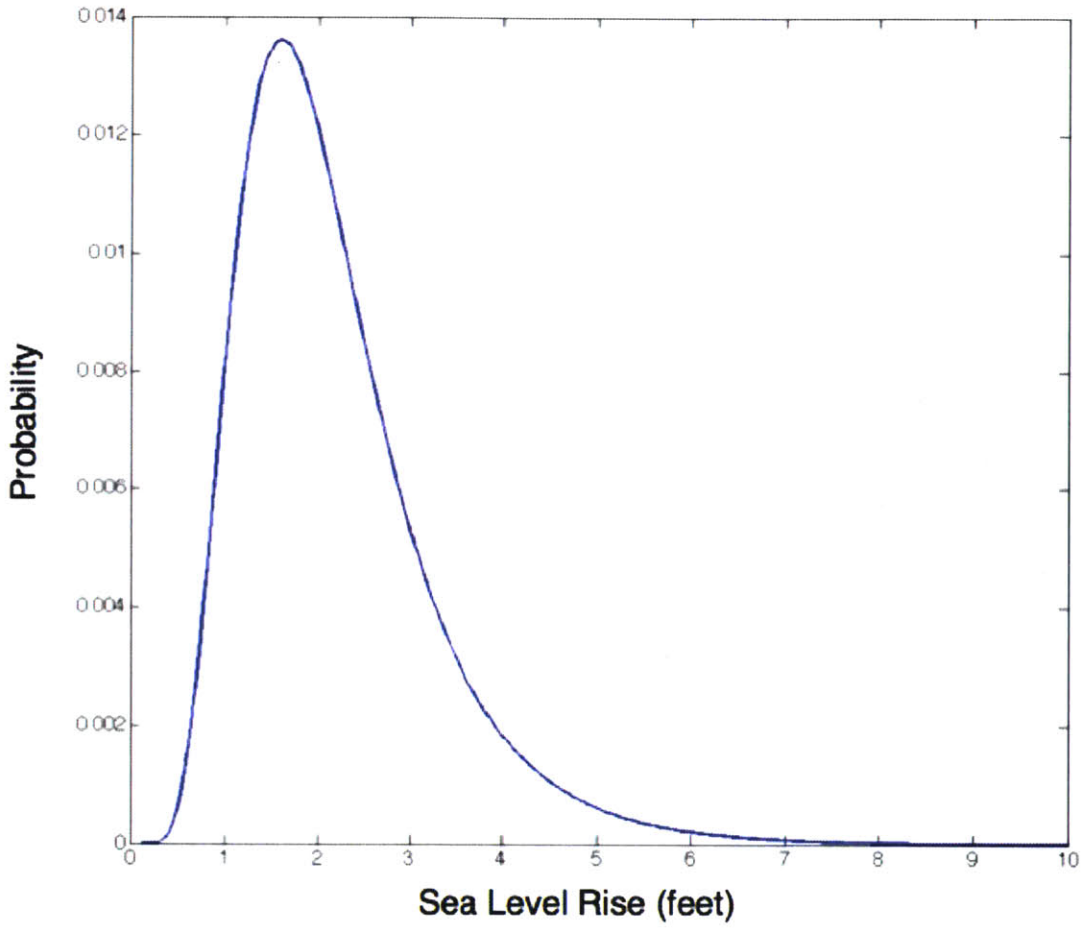

Figure 3-10: Lognormal distribution for sea level contributions from the Great Ice Sheets and West Antarctic Ice Sheet by 2100 with mean 0.6m and standard deviation of 0.14m.

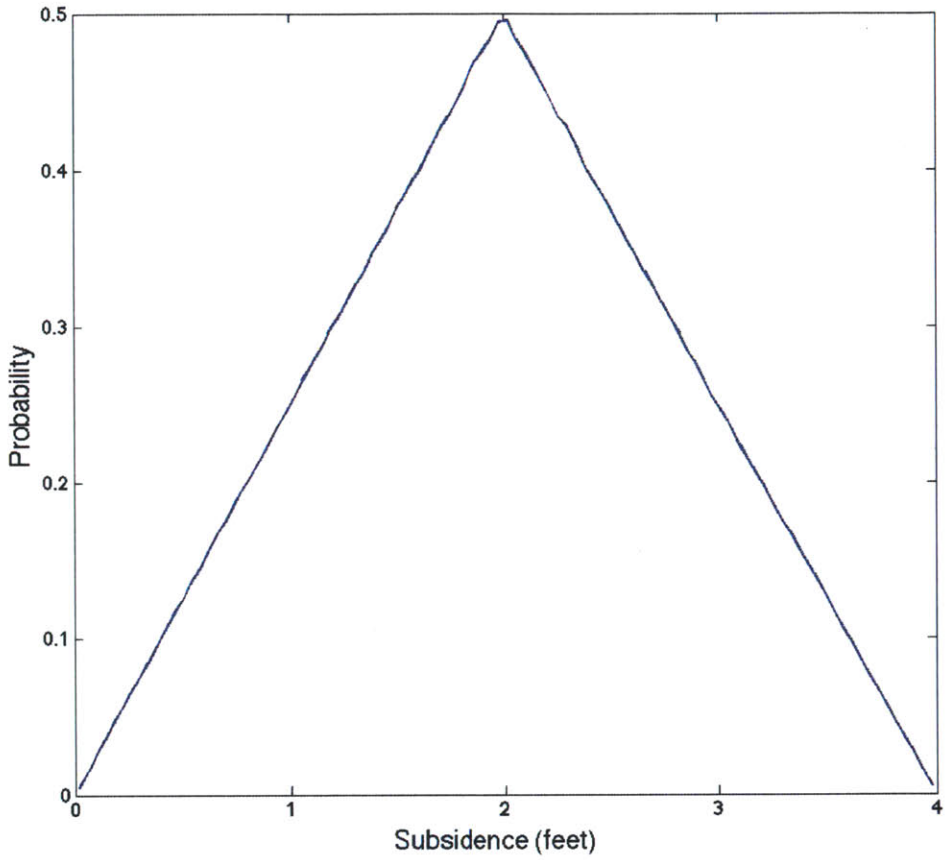

Figure 3-11: Triangular Distribution for subsidence levels in Galveston Bay, 2000 to 2100, with mean 2 feet, minimum 0 feet and maximum 4 feet.

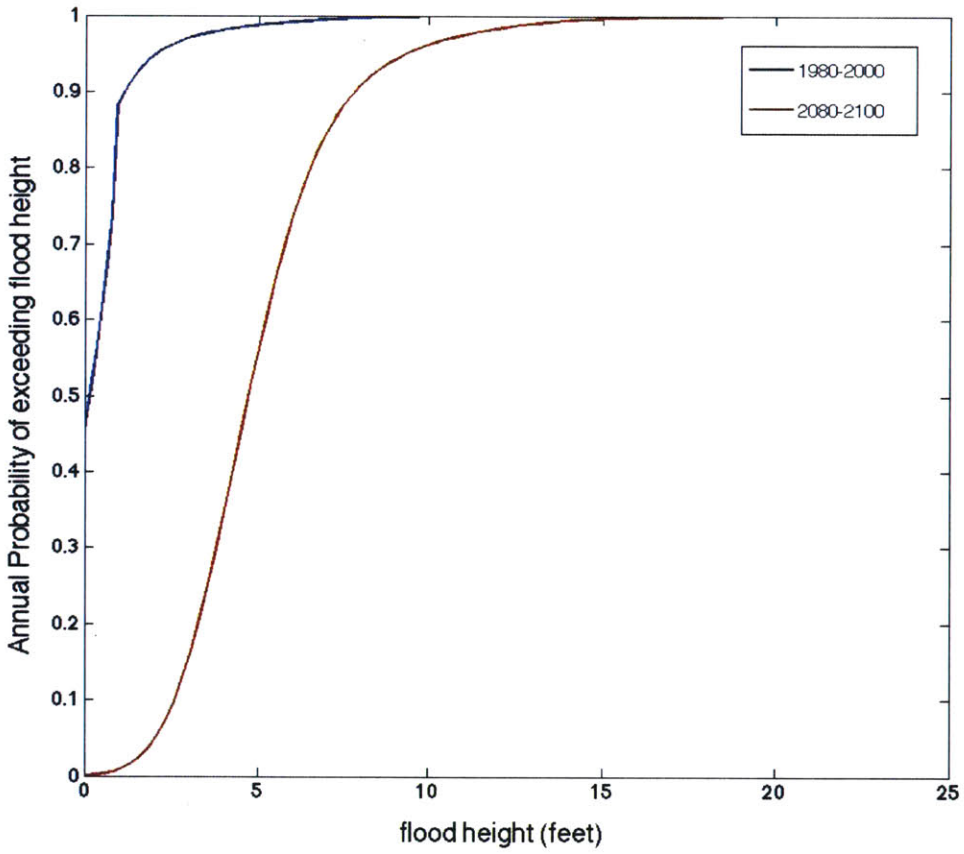

Figure 3-12: The resulting probability of inundation, including risks of storm surge, thermal expansion, sea level contributions from WAIS and GIS, and subsidence. The blue line is the probability distribution of inundation in 2000 and the red line is the probability distribution of inundation in 2100.

Chapter 4

Facility decision under risk

With events like the Fukushima Daiichi nuclear disaster or Hurricane Katrina's impact on the oil industry, we can understand how the security of our energy infrastructure has broad social, environmental, health, and economic implications. It's not always clear, however, whether a facility's risk is extreme enough to require adaptation to minimize losses and damages. In Chapter 4, we examine the decision making framework necessary to make the optimal adaptation strategy for coastal facilities that are vulnerable to flooding.

4.1 Translating Risks to Decisions

Each facility along the coast in Galveston is exposed to some risk of flood damage. In Chapter 3, we showed that for a facility at a 5 foot elevation along the coast, the risk of flooding, according to the GFDL model, and under 2000 climate conditions, is 1.27% and that by 2100 this risk is anticipated to increase to 47.16% under the assumptions outlined in Chapter 3. (Note that the risk analysis to be carried out in this chapter includes only the results from the GFDL model.) More generally, in Chapter 3 we also derived risk profiles for maximum yearly surge heights for both 2000 and 2100 climates. These risk profiles assume that no adaptation has taken place to date. As Galveston furthers the extent of its adaptation, however, we expect these risks to decrease.

In this analysis, adaptation in response to the risks of coastal flooding means the construction of levees or sea walls to retain ocean water. Levees are meant to minimize or

eliminate the impacts of storm surges and sea level rise on infrastructure up to a certain height. Levees do have the potential to fail, as was observed in New Orleans during Hurricane Katrina. Their effectiveness therefore relies on the integrity of the structures, which can be reinforced through time. In this analysis we assume no failure and further assume that once a levee is constructed, the maintenance of structure is maintained through time. A possible extension of this analysis would be to allow for the structure to degrade and/or fail and should be considered in future work. For the purposes of our analysis, we consider the major constraints in adaptation to be those imposed by the costs of building and the costs of maintaining the levee structure. There is the option to build a levee at any point in time or to add to an existing levee at any point in time. Here we build a dynamic programming model to identify the most economical adaptation strategy over time.

4.2 Adaptation Strategy: Dynamic Programming

As risks increase over time, there is a growing need for adaptation. The decision making process to adapt at any point in time depends on both the current risk a facility is exposed to and its expected future risk. Sequential decision making can add a complication to how we make decisions. Decisions made today will affect the future and therefore affect future decision making. Similarly, future possible decisions could affect what decisions we make today. Most crucial are the immediate decisions made so we construct our analysis to ultimately inform present day decisions.

In dynamic programming, during each time period, we consider the state of a facility and all possible decisions available within that state. For our analysis, the 'state' is the level of protection in place (i.e., the height of the levee in feet) and the decision 'action' options consist of the number of additional feet to build, including the option not to add any feet to the levee. The expected losses at any point in time is a function of future states and actions. We therefore begin optimizing in the last state and work our way backwards to our initial state. To limit the decision options we only consider adaptation options between 2000 and 2100, and we allow decisions for additional structures to be made at each decade (this means that the last state under consideration for decision making is the 2090-2100).

Further, we allow for up to a 20 foot tall levee to be added, as low as 0 feet, and on a 2 foot increment for options in between.

Define S_t and $A_t(S_t)$ to be the state and best action respectively at time t, and let $V_t(S_t)$ be defined as the lowest expected costs at time t in state S_t. Further, let $C_t(S_t, A_t)$ be the expected costs at time t given state S_t and action A_t.

For each time period, we calculate the best action and lowest value such that

$$A_t(S_t) = \arg\min_{A_t} \{C_t(S_t, A_t) + V_{t+1}(S_t + A_t)\}, \tag{4.1}$$

and

$$V_t(S_t) = \min_{A_t} \left\{ \frac{1}{(1+r)^t} (C_t(S_t, A_t) + V_{t+1}(S_t + A_t)) \right\}, \tag{4.2}$$

where r is the discount rate. $C_t(S_t, A_t)$ is defined as

$$C_t(S_t, A_t) = E(Damage|S_t, A_t) + c_m \times m \times S_t + c_b \times m \times A_t, \tag{4.3}$$

where $E(Damage|S_t, A_t)$ is the expected damage during the time period given the state and action, c_m is the cost of maintaining one foot-mile of sea wall, c_b is the cost of building an additional foot-mile of sea wall, and m is the number of miles of sea wall necessary to protect the facility.

Since we choose to look at decisions made every decade, each of these costs are accumulated over the decade, with the discount rate of r. We obtain probabilities of yearly inundation by interpolating between our two probability distributions shown in Figure 3-13. We interpolate the flood heights linearly between percentiles. For instance, if the 60^{th} percentile of flood heights is 0.5 feet in 2000 and 5.5 feet in 2100, then the 60^{th} percentile for the intermediate decades will be 1 foot in 2010, 1.5 feet in 2020, 2 feet in 2030 and so on. The underlying assumption for this interpolation is based on the linear relationship between sea level rise and temperature projections from the GCMs used from the IPCC under A1b, and a linear trend in temperature increases between 2000 and 2100. For the other components of the risk analysis (i.e. great ice sheets, subsidence, and hurricane intensity), there is lacking scientific understanding of the change in risk will progress over the century.

Due to the lacking scientific bases, our default assumption was a linear trend in a changing risk profile. Future work is needed to develop simulations for the intermediate decades between 2000 and 2100, but for now the resulting intermediate probability distributions are shown in Figure 4-1.

From these probability distributions, we can find $P_t(\zeta > \xi + S_t + A_t)$, which is the probability that the flood height, ζ, will exceed the wall height at elevation ξ in a given year with a protection height of $S_t + A_t$. To derive the expected damages over the t^{th} decade, we calculate

$$E(Damage|S_t, A_t) = \sum_{i=1}^{10} \frac{1}{(1+r)^{i-1}} \times D \times P_t(\zeta > \xi + S_t + A_t), \tag{4.4}$$

where D is the damage incurred by a flooded facility.

By iterating backwards over time, we are able to derive the optimal wall height for each state. We illustrate this method using a case of a flooded facility of similar magnitude to facilities that exist at 5 feet above today's mean sea level in Galveston. Costs incurred by this facility is the sum of lost or damaged infrastructure, loss of operational capacity until repairs were finished, and legal costs for damaged property as a result of the flood. Data is not available on potential damage to the refinery actually located at Point A in Galveston Bay, so to illustrate the method we assume the existence of a 200,000 barrel per day refinery at that point and apply estimates from a facility flooded by hurricane Katrina. The resulting model parameters are the following:

- D=$650,000,000
- c_m = $4330 per foot per mile[2]
- c_b = $1,000,000[3]
- $m = 5$ (number of miles of dykes required)

[2]The cost of annual levee maintenance per foot height per mile length is taken from Franck 2009(7). It's a rough estimate taken from Okita and Pritchard (2006) by averaging two levee projects there. The average was $4330 per ft per mile.

[3]Estimate based on public records of damage and liability costs of flooding, plus an estimate of the cost of almost a year's shutdown of a flooded refinery during Hurricane Katrina. The estimate is for illustrative purposes only and has not been reviewed or approved by the company.

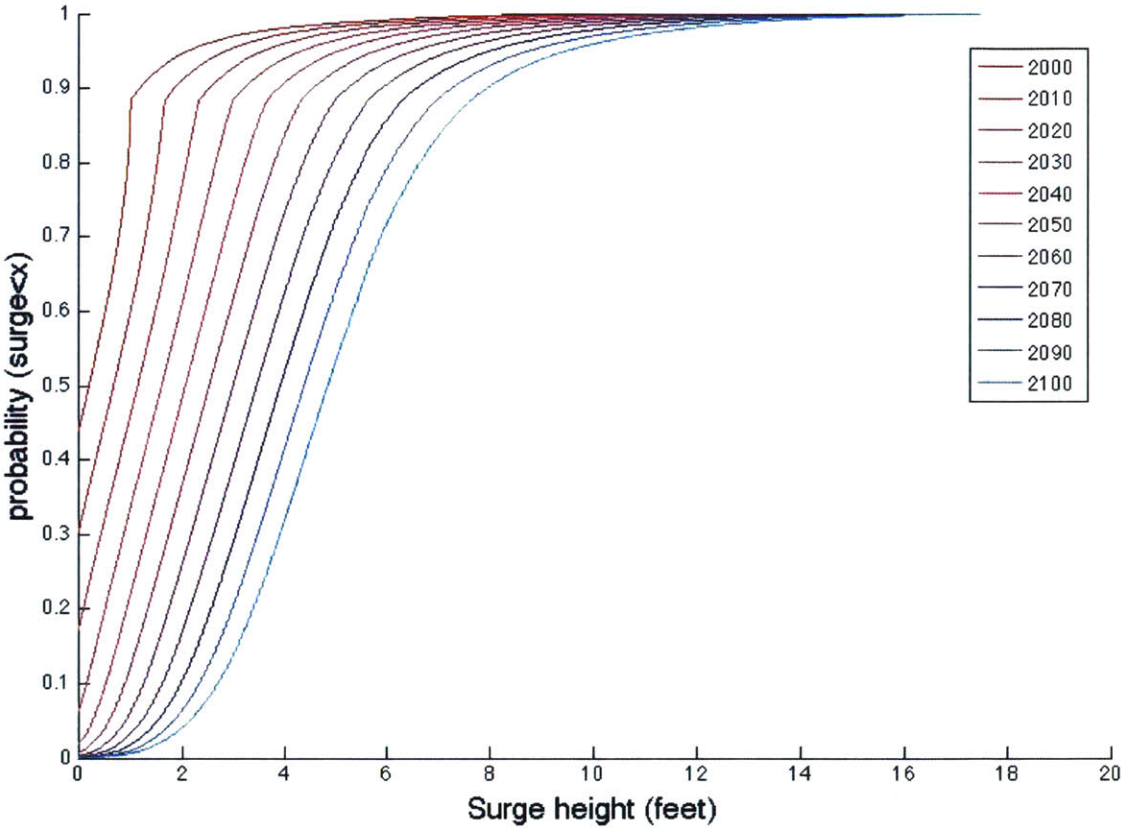

Figure 4-1: Probability distributions of inundation for each decade by interpolating between risk profiles from Figure 3-13

- $r = 0.05$
- $\xi = 5$ feet

The result is a decision matrix as shown in Figure 3-2 (need to format this matrix to be more clear).

	Year										
State (feet)	2000	2010	2020	2030	2040	2050	2060	2070	2080	2090	2100
0	8	8	8	8	10	10	10	12	12	12	12
2	8	8	8	8	10	10	10	12	12	12	12
4	8	8	8	8	10	10	10	12	12	12	12
6	8	8	8	8	10	10	10	12	12	12	12
8	8	8	8	8	10	10	10	12	12	12	12
10	10	10	10	10	10	10	10	12	12	12	12
12	12	12	12	12	12	12	12	12	12	12	12
14	14	14	14	14	14	14	14	14	14	14	14
16	16	16	16	16	16	16	16	16	16	16	16
18	18	18	18	18	18	18	18	18	18	18	18
20	20	20	20	20	20	20	20	20	20	20	20

Figure 4-2: Decision matrix for the height of sea wall recommended to minimize costs with a changing climate. The columns increase with each decade(2000, 2010, 2020,... 2100) and the rows increase indicating each state (0 feet, 2 feet, 4 feet, ... 20 feet)

With current projections of a changing climate over time, we produce a decision array that informs decisions sequentially over time. Note that this array will change as we further our understanding of the risks. To interpret the decision array, the columns move left to right with each decade, 1990-2000 being the first column. The rows are each state from 0 to 20 increasing with a step size of 2 feet. We can see that in the first row, (i.e. in a state with no protection) and first column (i.e. 1990-2000 time period), an 8 foot wall should be built immediately. If this decision is made then in the second decade (second column), at a state of 8 feet (5th row), no change in protection is called for. This remains true until the 5th time period when another 2 feet should be added for a total of a 10 foot levee. Following this decision path, the final construction is in adding another 2 feet in the 8th decade for a total of 12 feet.

The decision framework was also tested on a risk profile that remains constant over time, the profile identical to the 2000 climate. This means no changes in sea level or hur-

ricane activity would occur over a century. Regardless of this, the results still suggest to build a wall, but only one that is 6 feet in height (see Figure 4-3), 2 feet less than what our decision would be with a different future set of risks.

	Year										
State (feet)	2000	2010	2020	2030	2040	2050	2060	2070	2080	2090	2100
0	6	6	6	6	6	6	6	6	6	6	4
2	6	6	6	6	6	6	6	6	6	6	4
4	6	6	6	6	6	6	6	6	6	6	4
6	6	6	6	6	6	6	6	6	6	6	6
8	8	8	8	8	8	8	8	8	8	8	8
10	10	10	10	10	10	10	10	10	10	10	10
12	12	12	12	12	12	12	12	12	12	12	12
14	14	14	14	14	14	14	14	14	14	14	14
16	16	16	16	16	16	16	16	16	16	16	16
18	18	18	18	18	18	18	18	18	18	18	18
20	20	20	20	20	20	20	20	20	20	20	20

Figure 4-3: Decision matrix for the height of sea wall recommended to minimize costs with no changing climate. The columns increase with each decade(2000, 2010, 2020,... 2100) and the rows increase indicating each state (0 feet, 2 feet, 4 feet, ... 20 feet)

This decision framework allows us to see how postponing wall construction means that greater costs are absorbed in the future (see Figure 4-4) while exposing facilities to greater risks right now. This matrix displays the future expected accumulated costs in each period and in each state associated with making the optimal decision given the period and state (i.e. $C_t(S_t, A_t)$ from (4.3)). For instance, for 2000 in a state with no sea wall, if optimal decisions are made each decade, then the expected accumulated costs over the century are \$52.7 million (column 1, row 1). This framework also allows us to make sequential decisions in the situation where the optimal decision is infeasible at the given time period. If a wall is unaffordable today or if certain regulations restrict the construction of a wall now, we can still make near-optimal decisions in a subsequent decade in accordance with our analysis. For instance, if a sea wall can't be constructed in 2000 but is feasible in 2020, then the expected accumulated costs in 2020 will be \$50 million (column 3, row 1). Today's total expected costs, however, would also need to include the expected costs of no protection for the first two decades. Using risk profiles for 2000 and 2010 we calculate

the extra expected costs of leaving a facility unprotected and find that an additional $148 million dollars from expected damages would be incurred in that time frame.

This decision making framework provides us with useful insight in how to best adapt to climate change. Our decisions will be modified as the scientific understanding of risks evolve. But this decision making framework also allows us to decide if the costs of adaptation exceed the value of the facility. If today's net present value of an unprotected facility is greater than $52.7 million, then there are still financial gains of keeping the facility in operation. If, however, the net present value is less than $52.7 million, then the expected damages would outweigh the benefits of keeping the facility in operation. In this scenario, the optimal decision would be to abandon the facility.

	Year										
State (feet)	2000	2010	2020	2030	2040	2050	2060	2070	2080	2090	2100
0	52.7	51.2	50.4	49.8	49.3	48.8	48.5	47.5	46.6	44.7	41.1
2	43.2	42.2	41.8	41.6	41.5	41.4	41.5	48.0	10.2	38.5	35.2
4	33.7	33.2	33.2	33.4	33.7	34.0	34.4	34.1	33.7	32.4	29.4
6	24.2	24.1	24.6	25.3	25.9	26.5	27.3	27.3	27.3	26.3	23.6
8	14.8	15.1	16.0	17.1	18.1	19.1	20.2	20.6	20.9	20.2	17.8
10	7.48	7.58	8.09	8.97	10.3	11.7	13.1	13.8	14.5	14.1	11.9
12	3.60	3.47	3.51	3.74	4.23	5.1	6.13	7.10	8.08	8.0	6.13
14	2.10	1.85	16.8	1.58	1.56	1.6	1.80	2.17	2.60	3.0	2.59
16	1.92	1.62	13.8	1.20	1.05	0.93	0.83	0.75	0.68	0.63	0.60
18	2.10	1.76	15.0	1.29	1.11	0.97	0.84	0.72	0.60	0.46	0.28
20	2.30	1.93	16.4	1.41	1.22	1.05	0.92	0.79	0.65	0.50	0.30

Figure 4-4: Costs matrix (expressed as the net present value in that time period in $\$ \times 10^6$) for sea wall heights in each state and time period with optimal future decision making under changing climate. Note: costs correspond with sea wall heights from Figure 4-2

Chapter 5

Conclusions and Policy Recommendations

5.1 Summary

The effects of climate change have begun to take shape globally with changes in precipitation, milder winters, changes in storm patterns, warming oceans, and a rising sea level. For the coastal regions of the United States, there is increased concern of how sea level rise and storm patterns in particular, will expose the areas to greater threats of coastal flooding. In this work we present a methodology for modelling the changing vulnerability of coastal infrastructure in a changing climate with a first application to Galveston Bay energy facilities. The underlying assumption is that the future climate is a result of one emissions scenario, A1B, as defined by the IPCC AR4. We develop flood height probability distributions for each risk factor contributing to the threat of inundation. This includes:

1. Storm surges from hurricane simulations. A Coupled Hurricane Intensity Prediction System is run off of conditions from four distinct AOGCM results from the IPCC AR4 and the resulting hurricane simulations are applied to the SLOSH model to determine a resulting probability risk distribution for storm surge heights.

2. Sea level rise as a result of thermal expansion. We use a normal distribution based on six AOGCM sea level rise results under A1B from the IPCC AR4.

3. Sea level rise from the contributions of the Greenland and West Antarctic ice sheets. We derive a lognormal distribution based on a wide range of published results.

4. Subsidence as a result of the removal of groundwater or other resources. We use a triangular distribution which we estimate based on historical subsidence levels in the Galveston region.

We use a Monte Carlo method to randomly sample from each of these distributions in order to obtain a combined probability distribution for maximum yearly flood heights for both the 1980-2000 time period and the 2080-2100 time period.

We extend this analysis further to incorporate dynamic decision making under the changing risks of annual flooding. We interpolate between our 2000 and 2100 risk profiles to obtain intermediate risk distributions for each decade. For our decision analysis we choose a facility sitting at five feet above current mean sea levels in Galveston Bay and assume a similar damage potential as a 200,000 barrel per day refinery that was flooded during Hurricane Katrina. We consider the option to protect a facility by constructing sea walls, versus the option of leaving the facility unprotected. Through dynamic programming we derive the optimal decision making sequence for each decade in order to minimize total expected costs.
We find under our assumptions that for a facility at five feet above mean sea level, the annual risk of flooding today is about 1% and that this risk increases to somewhere between 38 and 47% by 2100.

This method provides an integrated risk assessment for facilities in Galveston Bay and would be a useful tool in determining the extent of protection that an operating facility could benefit from. This method can be more broadly applied to any coastal region with vulnerable infrastructure, or vulnerable assets by adjusting the probability distributions from the contributing factors to better reflect the impacts specific to those regions. The expected costs must also be adjusted to reflect the value of the facility under consideration.

5.2 Applications to Public Policy

As the nature of our weather patterns and environmental systems change, the policies governing human activities should be adjusted to reflect that change. Through our analysis, we've concluded that coastal energy infrastructure will become more vulnerable to inundation with a changing climate and contributing impacts of subsidence. Flood-related policies should therefore be developed to reflect this changing risk.

One of the major policy concerns with regards to coastal flooding is with regards to zoning and insurance policies. In 1965, Congress had passed the Southeast Hurricane Disaster Relief Act, which provided post-disaster relief following extreme floods. Shortly after this Act was passed, however, there was a call for a broader look at flood control in order to help mitigate future damage. In 1968, Congress created the National Flood Insurance Program (NFIP) to provide affordable flood insurance and provide floodplain management regulations to reduce the flood-damage potential in communities of high flood risk. NFIP is administered by the Federal Insurance and Mitigation Administration (FIMA) within the Federal Emergency Management Agency (FEMA) and is also responsible for administering programs aimed to provide assistance in reducing future damage in flood-prone regions. In order to be able to provide affordable insurance, the NFIP established a 100-year flood risk standard. Properties must meet this standard before qualifying for the subsidized insurance rates. Statistically, the 100-year standard means a 1% annual risk of flooding, therefore, "the 100-year flood has a 26 percent chance of occurring over the life of a 30-year mortgage"(6). If communities don't undertake mitigation efforts in compliance with the regulations established by NFIP, then they are not eligible for the subsidized insurance provided by FEMA.

One of FEMA's responsibilities is to deliver flood hazard maps of the Nations flood-prone regions. These maps are intended to identify regions at high-risk of flooding and to determine which zones fall under the 100-year standard. If sufficient precautionary measures are undertaken, such as the construction of a levee compliant with FEMA's criteria, then the risk maps are adjusted to take the alterations into account. This could mean that

properties would no longer be required by law to purchase flood insurance or that their insurance rates would decrease.

The hazards considered by FEMA are all based on todays vulnerable coastlines; they have not yet developed changing risks in to their models. For a 30-year mortgage, however, climate change is anticipated to change the risk established by FEMA today. Regions that may be in flood-prone areas in 30 years, may not realize how their risks and insurance costs may be liable to change. Incorporating a longer-term view in FEMAs flood mapping, will allow more informed decisions to be made regarding new developments. The methodology from this research could be applied to FEMA's map generation in order to provide better insight into the changing risks for property owners or developers.

Further attention should be paid to the contributing factors to increased risk of inundation. We highlight two of contributing factors here, the first being climate change. There exists a large body of literature that addresses the policy options and challenges for mitigating against future climate change outcomes. The scale of these policy options are considered on national and international platforms and while it is a critical topic that should not be overlooked, it is beyond the scope of our more regional analysis.

The second contributing factor to increased risk is subsidence, largely as a result of the removal of groundwater; the removal of minerals, oil or gas can also contribute to subsidence but groundwater removal has been noted to be the most crucial contributing factor in locations experiencing severe subsidence. If we look towards a favorable long-term outcome, we may be interested in developing policies to minimize the potential for subsidence. This could be restricting the rate of groundwater removal or replenishing the water table after the fact. The trouble with replenishing the water table is that a source of clean water is needed to replenish it with if we are to avoid contaminating the water supply. This would defeat the purpose, however, of removing water in the first place. Developing careful regulations for the amount and rate of ground-water removal is crucial to minimizing the subsidence rates in the United States.

Research has shown that decision makers' perception of risk is based on their rationality assumptions whereas investor's perception of risk is driven by their *perceived* storm risk (7). As we look to develop policies appropriate for changing risks, it is important that

decision makers are therefore well informed of the true changing risks. Further coastal analysis to the vulnerability to climate change would be needed to provide this insight.

5.3 Future Work

There are a number of components to this analysis that require improvements. The following are a few of the items that should be addressed in future work.

Modelling the changing environmental risks

- Expand emission scenarios to include more scenarios other than A1B which is under criticism for over-predicting short-term economic growth.

- The hurricane runs used for this analysis were based either on a climate from 1980-2000 or a climate from 2080-2100 under the A1B emissions scenario. To better understand how quickly hurricane magnitudes will change, it would be beneficial to run the hurricane model off of climates in the more immediate future, such as 2030 and 2050, to derive a more accurate path of the changing risks of inundation.

- The SLOSH model produces maximum surge heights within the boundaries of the coast but does not include inland elevation in the model. To more accurately predict the risk of flooding for low-lying facilities set inland, we should include topographic details and a wetting and drying factor into our surge model.

- The SLOSH model could not accommodate sea level rise or subsidence into the model prior to surge height predictions. To have more accurate predictions of surge heights over time, increased sea levels and/or subsiding coasts should be incorporated into the surge model to better reflect the combined impacts.

- The sea level probability distributions used in this analysis were derived from the best predictions available to us at the time of the study. As the science behind sea

level rise develops further, the probability distributions for sea level heights should be modified to better reflect these scientific developments.

- We included a triangular distribution for subsidence to indicate the major uncertainties in these predictions. Future work should involve subsidence models that incorporate potential policies to limit ground water extraction and better reflect the true risks of future subsidence.

- The analysis should be applied to different locations along the United States coast line. The features of Galveston make it specifically vulnerable and the severity of infrastructure vulnerability is anticipated to be less severe in different locations. Applying this methodology to different locations would give us a better idea of the degree to which other coastal infrastructure are exposed to increased threats of inundation. Given the complexity of this analysis, however, applications to different locations would be more feasible with the development of a reduced form model.

Infrastructure decision analysis

- In the dynamic decision making process, the options were to either continue with business as usual or adapt by constructing a sea wall. A third option would be to allow for abandonment in the decision making process. This option should be considered in future work.

- We've assumed in this analysis that once a levee is constructed that it is adequately maintained through time, indefinitely. In reality, there is the option to build a levee and not maintain it. This option should be considered in our analysis and would also impact the risk of failure. This risk of failure should therefore also be incorporated into the model and into the decision making process.

- Our analysis was based on existing infrastructure in Galveston Bay and neglected to incorporate potential future infrastructure in the region. To fully understand the true magnitude of future damage, we should better incorporate economic projections and future potential infrastructure into our analysis.

- The cost for adapting to a rising sea level was based on rough estimates and require validation both on the cost of constructing a sea wall (the cost is likely to vary depending on the location) and the cost of maintaining the sea wall (the cost is likely to vary depending on environmental conditions or quality of the initial construction).

Bibliography

[1] National Oceanic Atmospheric Administration. Hurricane basics. *U.S. Department of Commerce*, 1999.

[2] K.S. Bhat, M. Haran, A. Terando, and K. Keller. Climate projections using bayesian model averaging and space–time dependence. *Journal of Agricultural, Biological, and Environmental Statistics*, pages 1–23, 2011.

[3] A. Cazenave and W. Llovel. Contemporary sea level rise. *Annual Review of Marine Science*, 2:145–173, 2010.

[4] K. Emanuel. Increasing destructiveness of tropical cyclones over the past 30 years. *Nature*, 436(7051):686–688, 2005.

[5] K. Emanuel, R. Sundararajan, and J. Williams. Hurricanes and global warming. *Bull. Am. Meteorol. Soc*, 89:347–367, 2008.

[6] FEMA. Guidelines and specifications for flood hazard mapping partners, appendix d: Guidance for coastal flooding analyses and mapping. *Washington, DC: Federal Emergency Management Agency*, page 360, 2002.

[7] T.R. Franck. Coastal communities and climate change: A dynamic model of risk perception, storms, and adaptation. *PhD Dissertation, Massachusetts Institute of Technology*, page 422, 2009.

[8] D.L. Galloway, D.R. Jones, SE Ingebritsen, and Geological Survey (US). *Land subsidence in the United States*. US Geological Survey, 1999.

[9] J.L. Irish, D.T. Resio, and D. Divoky. Statistical properties of hurricane surge along a coast. *Journal of Geophysical Research*, 116(C10):C10007, 2011.

[10] B.R. Jarvinen, CJ Neuman, and MAS Davis. A tropical cyclone data tape for the north atlantic basin. *NOAA Tech. Memo. NWS NHC-22*, 1988.

[11] C.P. Jelesnianski, J. Chen, W.A. Shaffer, United States. National Oceanic, Atmospheric Administration, and United States. National Weather Service. *SLOSH: Sea, lake, and overland surges from hurricanes*. US Department of Commerce, National Oceanic and Atmospheric Administration, National Weather Service, 1992.

[12] L. Kantha. Time to replace the saffir-simpson hurricane scale. *Eos*, 87(1):3, 2006.

[13] T.R. Karl and K.E. Trenberth. Modern global climate change. *Science*, 302(5651):1719–1723, 2003.

[14] C.A. Katsman, W. Hazeleger, S.S. Drijfhout, G.J. van Oldenborgh, and G. Burgers. Climate scenarios of sea level rise for the northeast atlantic ocean: a study including the effects of ocean dynamics and gravity changes induced by ice melt. *Climatic Change*, 91(3):351–374, 2008.

[15] C.A. Katsman, A. Sterl, JJ Beersma, HW van den Brink, JA Church, W. Hazeleger, RE Kopp, D. Kroon, J. Kwadijk, R. Lammersen, et al. Exploring high-end scenarios for local sea level rise to develop flood protection strategies for a low-lying deltathe netherlands as an example. *Climatic change*, 109(3):617–645, 2011.

[16] B.D. Keim and R.A. Muller. *Hurricanes of the Gulf of Mexico*. Louisiana State Univ Pr, 2009.

[17] T.R. Knutson, J.L. McBride, J. Chan, K. Emanuel, G. Holland, C. Landsea, I. Held, J.P. Kossin, AK Srivastava, and M. Sugi. Tropical cyclones and climate change. *Nature Geoscience*, 3(3):157–163, 2010.

[18] N. Lin, K. Emanuel, M. Oppenheimer, and E. Vanmarcke. Physically based assessment of hurricane surge threat under climate change. *Nature Climate Change*, doi:10.1038/nclimate1389, in press, 2012.

[19] N. Lin, KA Emanuel, JA Smith, and E. Vanmarcke. Risk assessment of hurricane storm surge for new york city. *Journal of Geophysical Research*, 115(D18):D18121, 2010.

[20] RA Luettich Jr, JJ Westerink, and N.W. Scheffner. Adcirc: An advanced three-dimensional circulation model for shelves, coasts, and estuaries. report 1. theory and methodology of adcirc-2ddi and adcirc-3dl. Technical report, DTIC Document, 1992.

[21] J.X. Mitrovica, M.E. Tamisiea, J.L. Davis, and G.A. Milne. Recent mass balance of polar ice sheets inferred from patterns of global sea-level change. *Nature*, 409(6823):1026–1029, 2001.

[22] R.J. Nicholls and A. Cazenave. Sea-level rise and its impact on coastal zones. *Science*, 328(5985):1517–1520, 2010.

[23] Committee on America's Climate Choices. *America's Climate Choices*. National Academies Press, 2011.

[24] R.A. Pielke Jr, J. Gratz, C.W. Landsea, D. Collins, M.A. Saunders, and R. Musulin. Normalized hurricane damage in the united states: 1900–2005. *Natural Hazards Review*, 9:29, 2008.

[25] S. Rahmstorf. A semi-empirical approach to projecting future sea-level rise. *Science*, 315(5810):368–370, 2007.

[26] J.L. Rego and C. Li. Nonlinear terms in storm surge predictions: Effect of tide and shelf geometry with case study from hurricane rita. *Journal of Geophysical Research*, 115(C6):C06020, 2010.

[27] S. Solomon, G.K. Plattner, R. Knutti, and P. Friedlingstein. Irreversible climate change due to carbon dioxide emissions. *Proceedings of the national academy of sciences*, 106(6):1704, 2009.

[28] S. Solomon, D. Qin, M. Manning, Z. Chen, M. Marquis, K.B. Averyt, M. Tignor, , and ed. Miller, H.L. Climate change 2007: The physical science basis. *International Panel on Climate Change*, Fourth Assessment Report, 2007.

[29] DOE US. Total energy production. *Energy Information Administration, Annual Energy Outlook*, 2009.

[30] M. Vermeer and S. Rahmstorf. Global sea level linked to global temperature. *Proceedings of the National Academy of Sciences*, 106(51):21527–21532, 2009.

[31] P.J. Webster, G.J. Holland, J.A. Curry, and H.R. Chang. Changes in tropical cyclone number, duration, and intensity in a warming environment. *Science*, 309(5742):1844–1846, 2005.

[32] R.H. Weisberg and L. Zheng. Hurricane storm surge simulations for tampa bay. *Estuaries and Coasts*, 29(6):899–913, 2006.

[33] D. Yergin. Ensuring energy security. *Foreign Affairs*, 85(2):69–82, 2006.